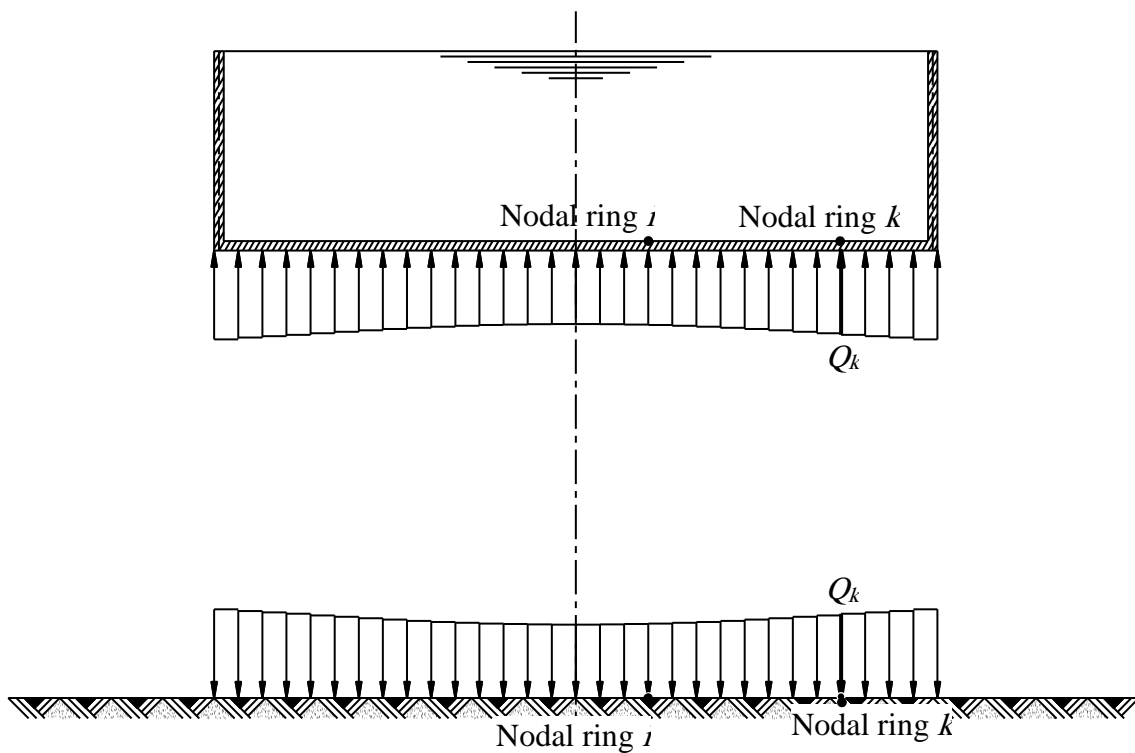


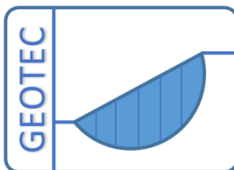
# Analysis of Axisymmetric Structures and Tanks by the Program *ELPLA*

## Part I: Numerical models



*M. El Gendy*

*O. El Gendy*



Copyright ©

GEOTEC Software Inc.

PO Box 14001 Richmond Road PO, Calgary AB, Canada T3E 7Y7

Tele.:+1(587) 332-3323

[geotec@geotecsoftware.com](mailto:geotec@geotecsoftware.com)

[www.geotecsoftware.com](http://www.geotecsoftware.com)

Table of Contents	Page
<b>1 Mathematical model.....</b>	<b>1-4</b>
1.1 Introduction .....	1-4
1.2 Axi-symmetric shells of revolution.....	1-6
1.2.1 Introduction .....	1-6
1.2.2 Excerpt from the theory of shells of revolution .....	1-6
1.2.3 External loads .....	1-9
1.2.4 Internal forces.....	1-9
1.2.5 Shells of revolution geometry .....	1-11
1.3 Analytical solution of circular cylindrical shells.....	1-16
1.3.1 Introduction .....	1-16
1.3.2 General equation of circular cylindrical shell .....	1-16
1.3.3 Boundary conditions .....	1-17
1.3.4 Internal forces.....	1-18
1.4 Finite elements analysis of axi-symmetric shells of revolution .....	1-19
1.4.1 Introduction .....	1-19
1.4.2 Nodal vectors of displacements and forces.....	1-19
1.4.3 Displacement function.....	1-22
1.4.4 Displacement transformation from local to global co-ordinates .....	1-23
1.4.5 Strain-displacement formulation .....	1-25
1.4.6 Stress-displacement formulation .....	1-27
1.4.7 Stiffness matrix formulation.....	1-28
1.4.8 Calculation process with axially symmetrical loading.....	1-31
1.4.9 Simulation of circular plate .....	1-32
1.4.10 Simulation of the tank wall and base using thin shell element .....	1-33
1.5 Analysis of water tanks under static loading.....	1-35
1.5.1 Introduction .....	1-35
1.5.2 Simple assumption model .....	1-37
1.5.3 <i>Winkler's</i> model.....	1-39
1.5.4 <i>Winkler's/</i> Continuum model .....	1-42
1.5.5 Continuum model for elastic base .....	1-46
1.5.6 Continuum model for rigid base.....	1-50
1.5.7 Continuum model for flexible base .....	1-52
1.6 Preference.....	1-54

## Preface

Various problems in geotechnical Engineering can be investigated by the program *ELPLA*. The original version of *ELPLA* was developed by the father of elastic foundation Prof. M. Kany, Prof. M. El Gendy and Dr. A. El Gendy. After the death of Prof. Kany, Prof. M. El Gendy and Dr. A. El Gendy further developed the program to meet the needs of practice.

This book describes procedures and methods available in *ELPLA* to analyze circular cylindrical shells structures. It is also considered, circular cylindrical tank resting on any layered compressible soil as one unit taking into account the soil-structure interaction effect.

The purpose of this text is to present the methods, equations, procedures, and techniques used in the formulation and development of the *ELPLA* function for analyzing tanks on different subsoil models. It is of value to be familiar with this information when using the software.

An understanding of these concepts will be of great benefit in applying the software, resolving difficulties and judging the acceptability of the results.

Two familiar types of subsoil models are considered, *Winkler's* model and Continuum model. In addition, the simple assumption model is also considered. This model assumes linear contact pressure on the base of the tank.

The mathematical solution of the circular cylindrical tanks is based on the Finite Element Method using axi-symmetric circular cylindrical shell elements.

In which, axi-symmetric shell finite elements represent the tank wall and tank base according to the nature geometry of the structure.

Based on his M.Sc. research, *El Gendy, O. (2016)* had carried out a numerical modification on the methods in *ELPLA* for analyzing rafts to be applicable for analyzing cylindrical water storage tanks. Many tested examples are presented to verify and illustrate the available methods. Some of verification examples for analyzing cylindrical water storage tanks on multi-layered soil carried out by *El Gendy, O. (2016)* are presented in the second part of this book.

## 1 Mathematical model

### 1.1 Introduction

In this book, the structural behavior of circular cylindrical tanks resting on any layered compressible soil is investigated. In the developed mathematical models, tanks are subjected to static loading. Most of all numerical models of this research are new introduced in the program *ELPLA* 12 [13]. *ELPLA* was developed before to analyze floor slabs, shear walls, grids, frames, rafts and piled rafts using beam and plate elements as shown in Figure 1.1. Figure 1.2 shows the recent version of *ELPLA* 12 including the new aspect concerning the icon "Analysis of rotational shells". An axi-symmetric shell finite element formulation is added to analyze circular cylindrical tanks. The idea of using axi-symmetric shell finite element is to simulate the tank wall, tank base and subsoil as one unit taking into account the soil-structure interaction effect. Using the conditions of axial symmetry, enables to convert the completed three-dimensional problem of super structure, foundation and soil into axi-symmetry problem. Base of the tank may be considered as rigid, elastic or flexible. For analyzing the base of the tank as elastic base, full compatibility between the structure elements and subsoil is occurred.

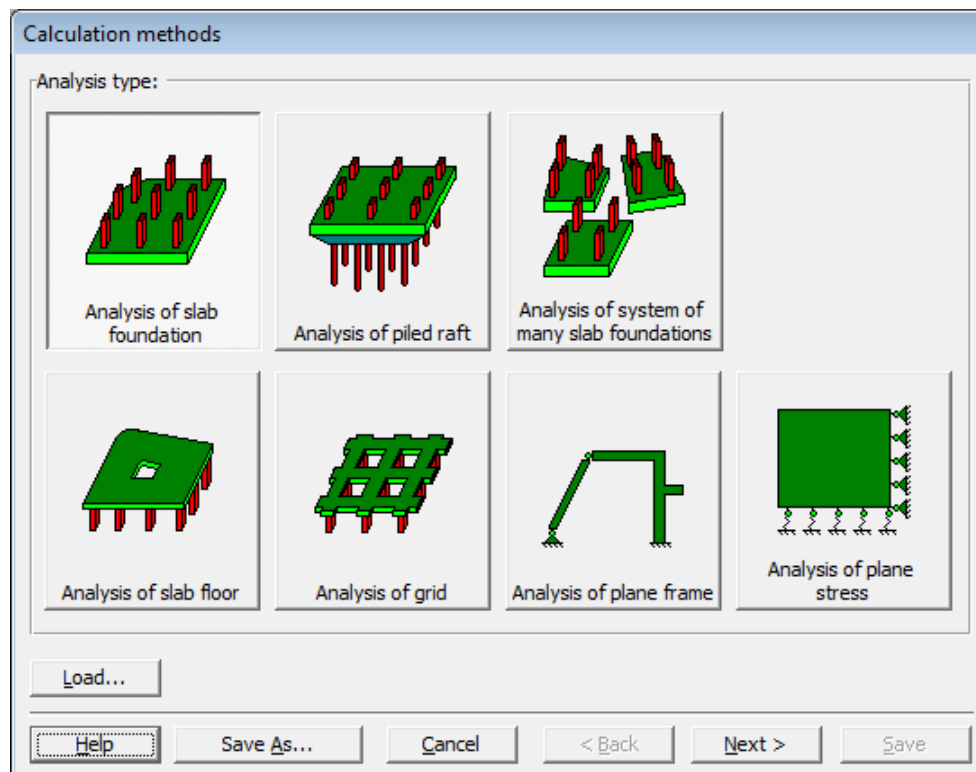


Figure 1.1 Aspects treated in *ELPLA* 11

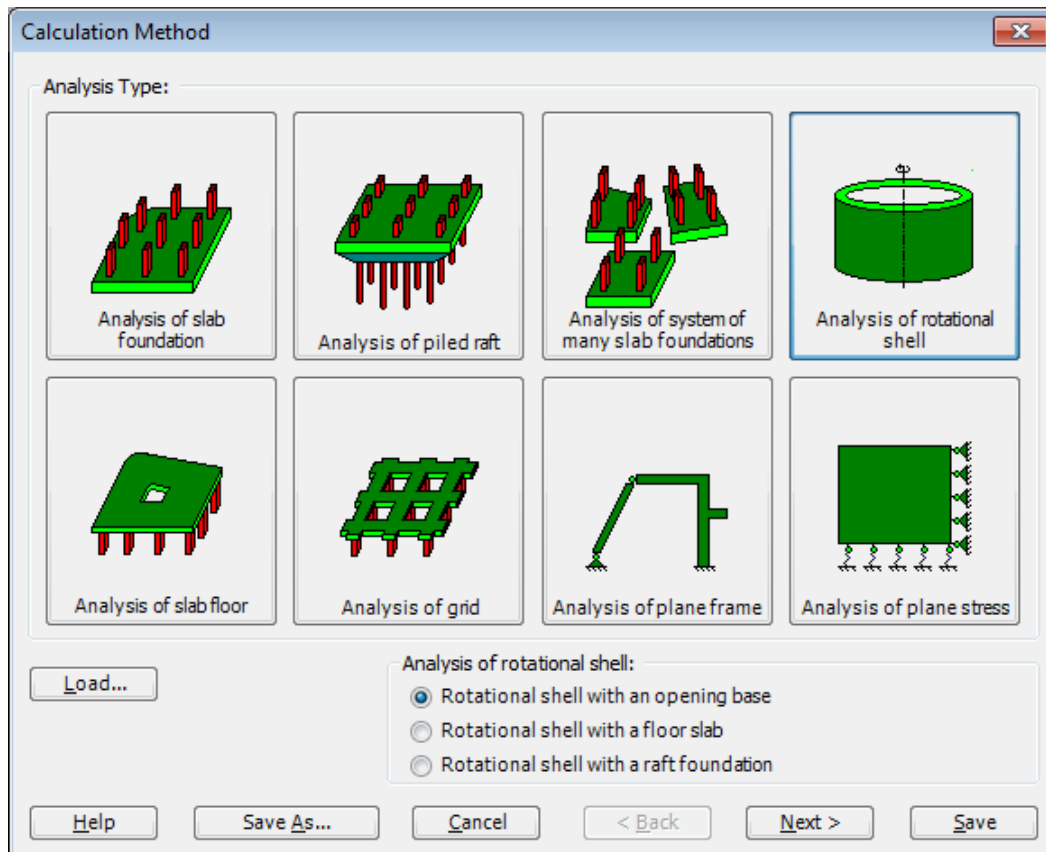


Figure 1.2 Aspects treated in *ELPLA 12*

## 1.2 Axi-symmetric shells of revolution

### 1.2.1 Introduction

Circular cylindrical shells analysis may be considered as an axi-symmetric shell structure problem. An axi-symmetric shell structure can be idealized by a series of conical frustum-shaped elements as shown in Figure 1.7. This element was first suggested by *Grafton and Strome* (1963) and later its use was extended by *Percy et al* (1965). It may be noted that this single element has two ring nodes. Since both in-plan and out of plan displacements and forces have to be considered in shell structures, the displacement vector for each node contains axial and radial movements as well as rotation as shown in Figure 1.7 - b). Finite element analysis of axi-symmetric shells in the simplified approach of *Grafton and Strome* (1963) are presented by many authors. Some of them are *Zienkiewicz/ Taylor* (1967), *Rockey et al* (1975), *Szilard* (1986), and *Melerski* (2000). *Szilard* (1986) presented a more extensive analysis of axi-symmetric shell structure with a computer program code. The following steps of the FE analysis of axi-symmetric shell structure depends on that of *Rockey et al* (1975) and *Szilard* (1986).

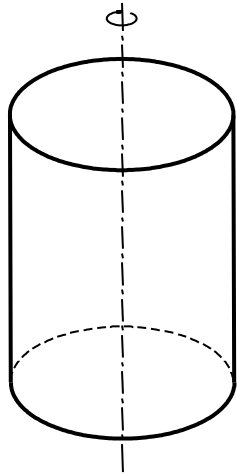
### 1.2.2 Excerpt from the theory of shells of revolution

The axi-symmetric shells of revolution are thin-walled shell structures, which are curved in one or two mutually perpendicular directions. The average surface of a rotating shell is formed by rotating a plane curve about a horizontal axis in its plane of rotation as shown in Figure 1.4 a). If the meridian curve for example a circle, an ellipse or a parabola, then shells are generated of revolution in the form of a sphere, a paraboloid or an ellipsoid. In construction, these shells are used as warehouses, tanks, towers, silos, etc.

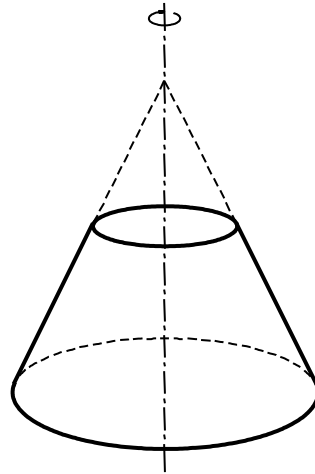
For the exposure provided in this research that they constantly and also axi-symmetric. The symmetry of the shell and the load allows it to perform the calculation in two dimensions.

The theory of axi-symmetric shells is based on the following assumptions:

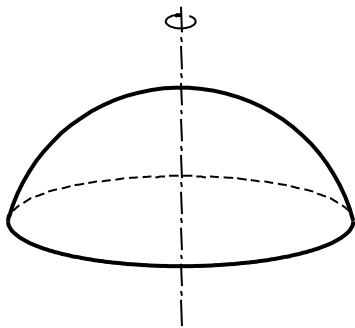
- The shell thickness is small compared to the other dimensions.
- The deformation is small, so the influence of shape changes on the distribution of forces are negligible.
- The claimed cross-sections remain plane in bending.
- The material is isotropic and linear elastic.



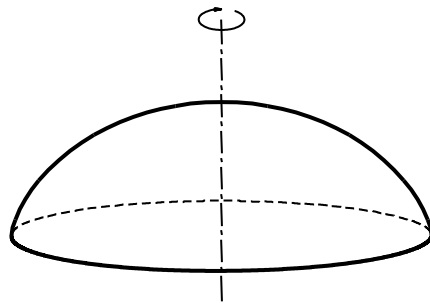
Circular cylindrical shell



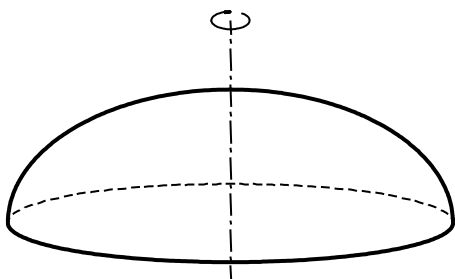
Conical shell



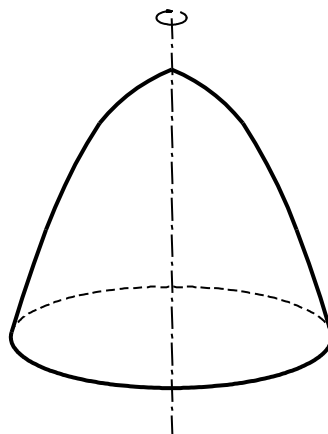
Spherical shell



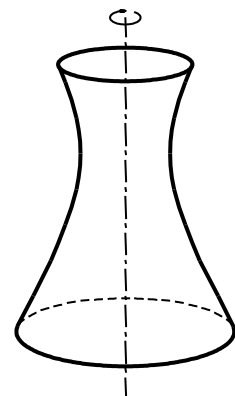
Cycloidal shell



Elliptical shell



Parabolic shell



Hyperbolic shell

Figure 1.3 Applications of axi-symmetric shell structures

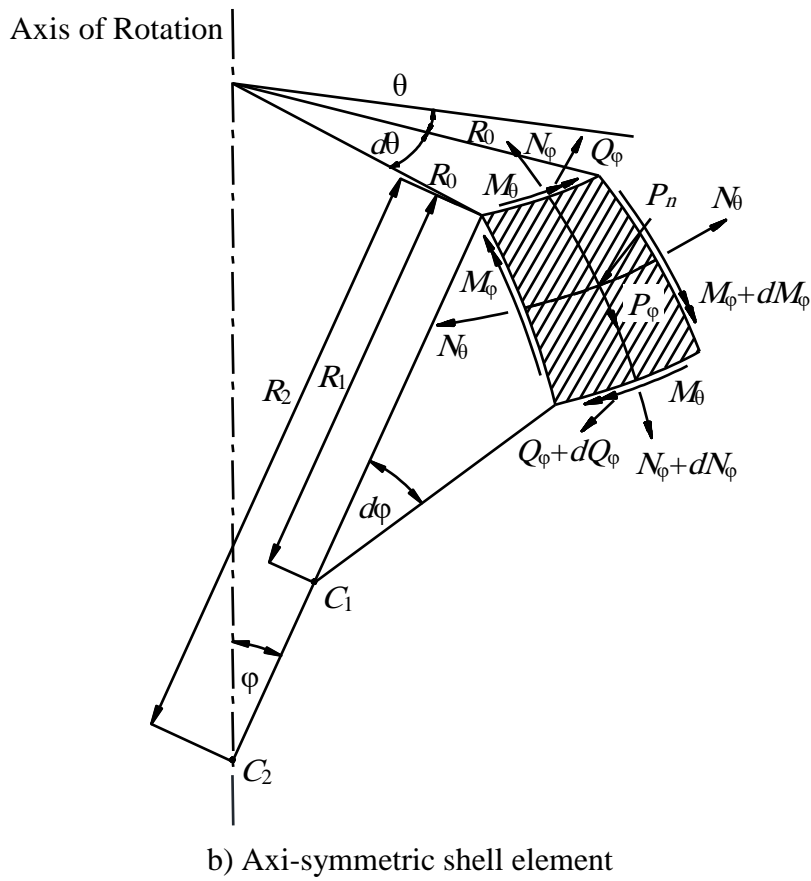
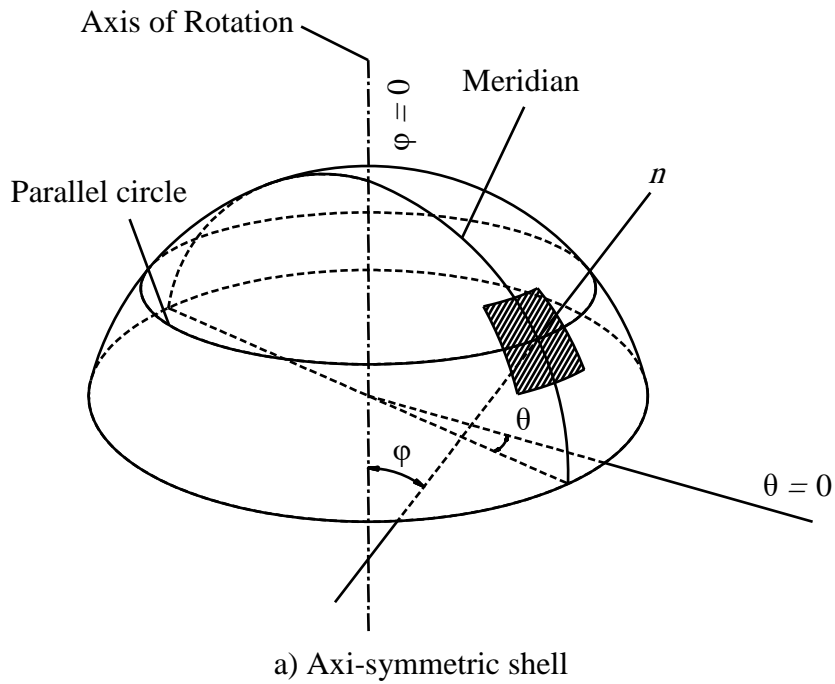


Figure 1.4 Shell element subjected to axi-symmetric loading

In the practical solution of axi-symmetrically loaded shells, the following external loads are considered:

- Own weight
- Live load
- Liquid pressure
- Earth pressure
- Gas pressure
- Lateral loads like wind, earthquakes, etc.

### 1.2.3 External loads

The load  $P$  per unit area that acts on the shell element is analyzed into two component (Figure 1.4 b)):  $P_\varphi$  acts in the meridional direction and  $P_n$  acts in the direction normal to the surface. The load component  $P_\theta$  is in any case zero due to the axi-symmetry of the shell.

### 1.2.4 Internal forces

The internal forces generated by the axi-symmetric loading are shown in Figure 1.4 b) with its positive directions. In addition to the membrane forces  $N_\varphi$  and  $N_\theta$ , the components  $Q_\varphi$ ,  $M_\varphi$  and  $M_\theta$  act in the bending state.

In the most general case, each side of an element cut out of a thin shell is acted upon by five kinds of internal actions, namely

- 1- Normal Forces ( $N_\varphi$ ,  $N_\theta$ ).
- 2- Tangential (in-plan) shearing force ( $N_{\theta\varphi}$ ,  $N_{\varphi\theta}$ ).
- 3- Transverse (normal) shearing force ( $Q_\varphi$ ,  $Q_\theta$ ).
- 4- Bending moments ( $M_\varphi$ ,  $M_\theta$ ).
- 5- Torsional Moments ( $M_{\varphi\theta}$ ,  $M_{\theta\varphi}$ ).

In an axi-symmetric system of loading, the transverse shearing force component ( $Q_\theta$ ), the tangential shearing force components ( $N_{\theta\varphi}$ ,  $N_{\varphi\theta}$ ) and torsional moments ( $M_{\varphi\theta}$ ,  $M_{\theta\varphi}$ ) are not available. According to the approximation of *Geckeler* (1930) and the references of *Timoshenko/ Woinowsky* (1959), *Bakhoun* (1992) and *Ventsel/ Krauthammer* (2001), the equilibrium conditions can be written in a simplified form as:

$$\left. \begin{aligned} \frac{\partial}{\partial \varphi} (N_\varphi R_o) - N_\theta R_1 \cos \varphi - Q_\varphi R_o + P_\varphi R_1 R_o &= 0 \\ \frac{\partial}{\partial \varphi} (Q_\varphi R_o) + N_\varphi R_o + N_\theta R_1 \sin \varphi + P_n R_1 R_o &= 0 \\ -\frac{\partial}{\partial \varphi} (M_\varphi R_o) + M_\theta R_1 \cos \varphi + Q_\varphi R_1 R_o &= 0 \end{aligned} \right\} \quad (4.1)$$

where:

- $R_0$  The radius of the parallel circle, [m].
- $R_1$  The principal radius of curvature of a shell in the meridional plan, [m].
- $R_2$  The principal radius of curvature of a shell in the normal plan, [m].
- $\varphi$  The meridional angle formed by the extended normal to the surface and the axis of rotation. All points of a parallel circle make the same angle, [°].
- $\theta$  The circumferential angle that a meridian make with the reference meridian ( $\theta = 0$ ) along the parallel circle, [°].

These three equations contain five unknowns, so the problem is internally statically indeterminate. To calculate the internal forces  $N_\varphi$ ,  $N_\theta$ ,  $M_\varphi$ , and  $M_\theta$ , the membrane forces and the bending moments are expressed as functions of the displacements  $u$  and  $w$ :

$$\left. \begin{aligned} N_\varphi &= \frac{Et}{1-\nu^2} \left[ \frac{1}{R_1} \left( \frac{du}{d\varphi} - w \right) + \frac{\nu}{R_2} (u \cot \varphi - w) \right] \\ N_\theta &= \frac{Et}{1-\nu^2} \left[ \frac{1}{R_2} (u \cot \varphi - w) + \frac{\nu}{R_1} \left( \frac{du}{d\varphi} - w \right) \right] \\ M_\varphi &= -D \left[ \frac{1}{R_1} \frac{d}{d\varphi} \left( \frac{u}{R_1} + \frac{1}{R_1} \frac{dw}{d\varphi} \right) + \frac{\nu}{R_2} \left( \frac{u}{R_1} + \frac{1}{R_1} \frac{dw}{d\varphi} \right) \cot \varphi \right] \\ M_\theta &= -D \left[ \frac{1}{R_2} \left( \frac{u}{R_1} + \frac{1}{R_1} \frac{dw}{d\varphi} \right) \cot \varphi + \frac{\nu}{R_1} \frac{d}{d\varphi} \left( \frac{u}{R_1} + \frac{1}{R_1} \frac{dw}{d\varphi} \right) \right] \end{aligned} \right\} \quad (4.2)$$

where:

- $E$  Young's modulus of the shell material, [kN/m<sup>2</sup>].
  - $\nu$  Poisson's ratio of the shell material, [-].
  - $t$  Shell thickness, [m].
  - $u$  Displacement component in the meridional direction, [cm].
  - $w$  Displacement component in the direction normal to the middle surface, [cm].
- and, the flexural rigidity  $D$  is:

$$D = \frac{Et^3}{12(1-\nu^2)} \quad (4.3)$$

Figure 1.5 show the position of the shell part  $AB$  before and after deformation, considering the displacement components  $u$  and  $w$  in meridional and normal directions, respectively.

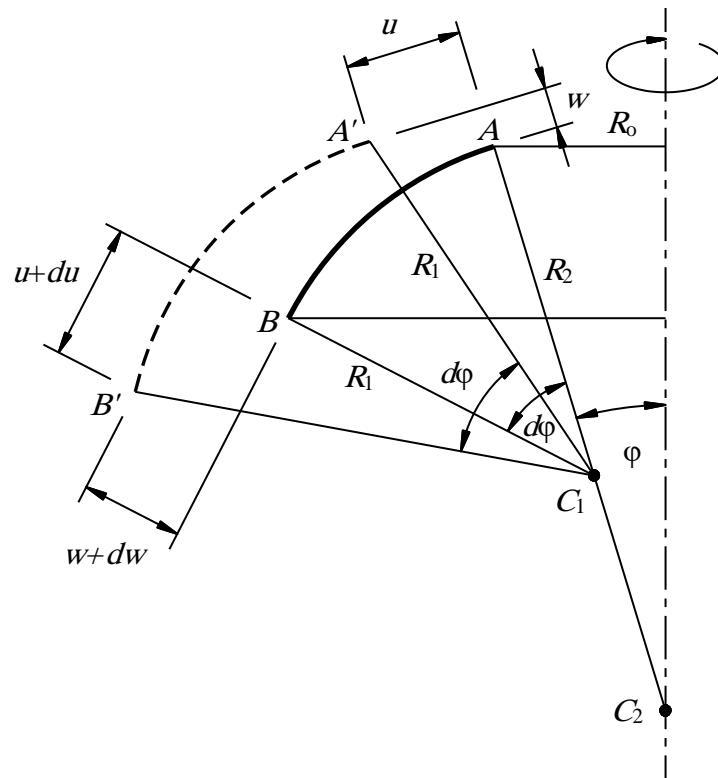


Figure 1.5 Shell displacement components  $u$  and  $w$

### 1.2.5 Shells of revolution geometry

Table 1.1 show the geometry parameters of some types of shells of revolution. These parameters are the meridian curve equation, the maximum and minimum principal radii of curvature equations and the meridional or tangential angle equation.

The meridional angle or the angle of the tangent can be written as:

$$\tan \phi = \frac{dz}{dr} \quad (4.4)$$

The principal radius of curvature of the meridian can be written as:

$$R_1 = \frac{1}{\kappa_1} = - \frac{\left(1 + \left(\frac{dr}{dz}\right)^2\right)^{3/2}}{\frac{d^2 r}{dz^2}} \quad (4.5)$$

## Mathematical model

---

The principal radius of curvature of the parallel circle can be written as:

$$R_2 = \frac{1}{\kappa_2} = r \left( 1 + \left( \frac{dr}{dz} \right)^2 \right)^{1/2} \quad (4.6)$$

where

$\kappa_1$  the curvature in the meridional direction.

$\kappa_2$  the curvature in the normal plan perpendicular to the meridian.

The principal radii of curvature for convex shells of revolution formed by rotating curves of the second order about their axes of symmetry can also be computed from the following equations:

$$R_1 = \frac{r_0}{(1 + \zeta \sin^2 \varphi)^{3/2}}, R_2 = \frac{r_0}{(1 + \zeta \sin^2 \varphi)^{1/2}} \quad (4.7)$$

Where the parameter  $r_0$  equals the value of the radii of curvature at  $\varphi = 0$ , i.e., at the vertex of the corresponding shell, and the parameter  $\zeta$  takes on the following values:

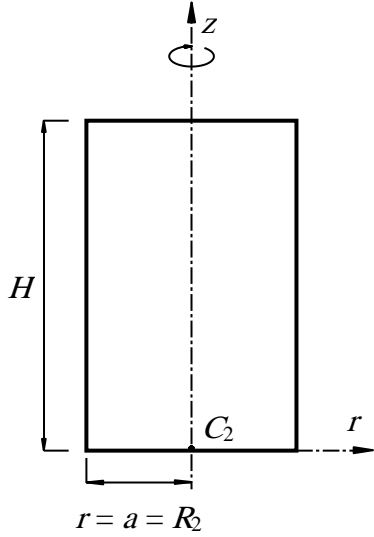
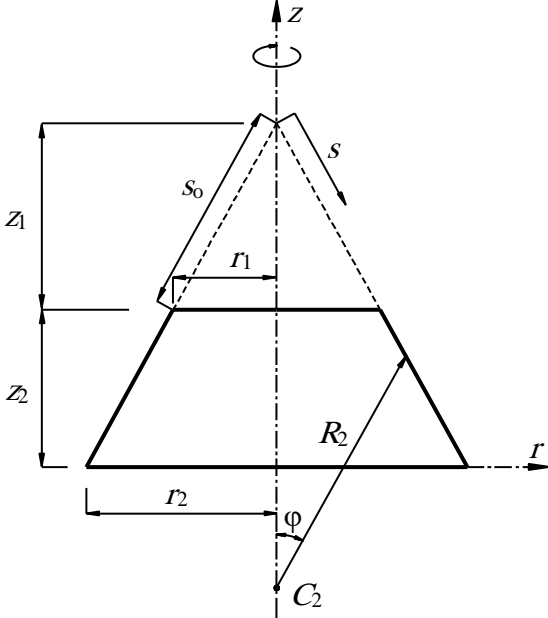
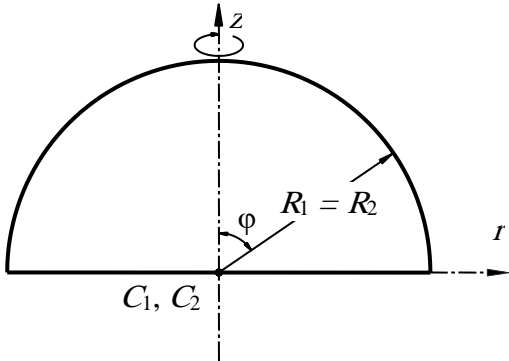
$\zeta = 0$  for a spherical shell;

$\zeta = -1$  for paraboloids;

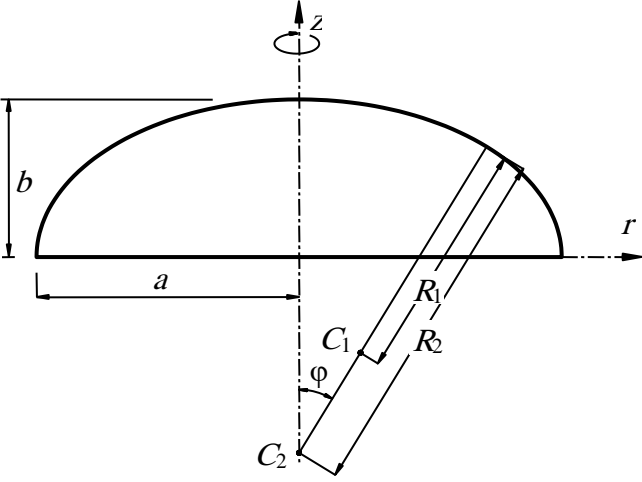
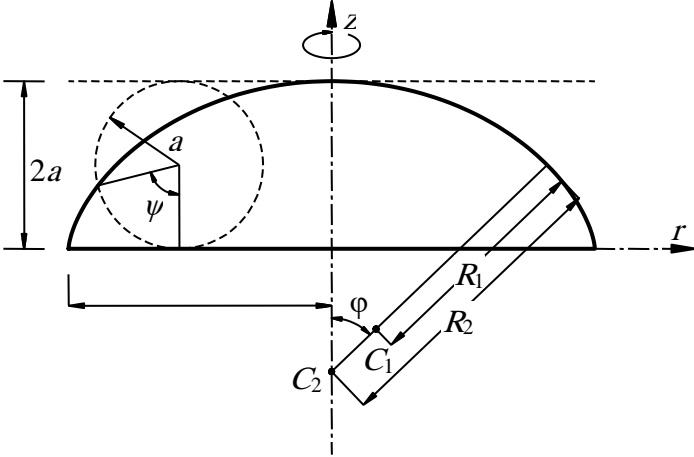
$\zeta > -1$  for ellipsoids and cycloids;

$\zeta < -1$  for hyperboloids.

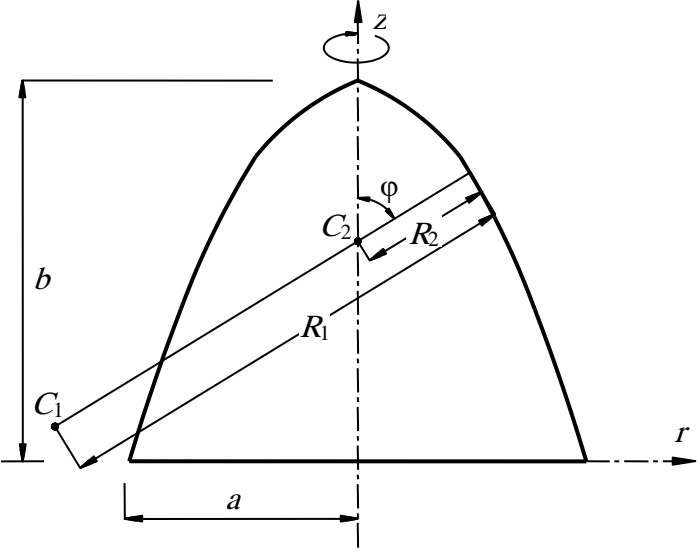
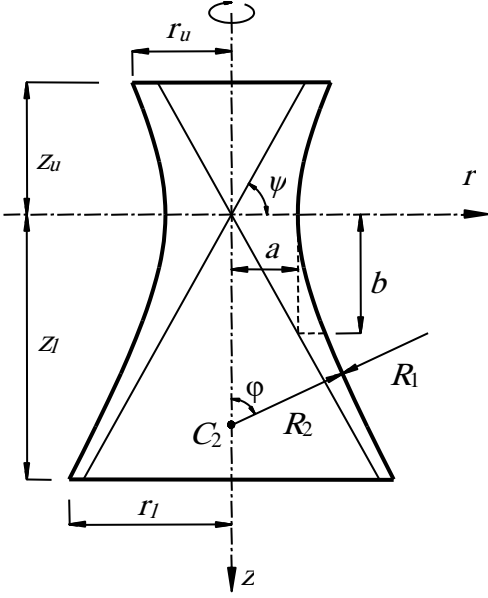
Table 1.1 Types of shells of revolution

Shell Geometry	Parameters
 <p style="text-align: center;"><math>r = a = R_2</math></p>	<p style="text-align: center;"><b><u>Cylindrical shell</u></b></p> <p style="text-align: center;"><math>r = a = R_2</math></p> <p style="text-align: center;"><math>R_1 = \infty</math></p> <p style="text-align: center;"><math>\varphi = 0</math></p>
	<p style="text-align: center;"><b><u>Conical shell</u></b></p> <p style="text-align: center;"><math>r = r_2 - \left(\frac{r_2 - r_1}{z_2}\right) z = r_2 - z \tan \varphi</math></p> <p style="text-align: center;"><math>R_1 = \infty</math></p> <p style="text-align: center;"><math>R_2 = s \cot \varphi</math></p> <p style="text-align: center;"><math>\varphi = \tan^{-1} \left(\frac{r_2 - r_1}{z_2}\right)</math></p>
	<p style="text-align: center;"><b><u>Spherical shell</u></b></p> <p style="text-align: center;"><math>z^2 + r^2 = a^2</math></p> <p style="text-align: center;"><math>R_1 = R_2 = a</math></p> <p style="text-align: center;"><math>\varphi = \tan^{-1} \left(\frac{r}{z}\right)</math></p>

Continue Table 1.1 Types of shells of revolution

Shell Geometry	Parameters
	<p><b><u>Elliptical shell</u></b></p> $\frac{r^2}{a^2} + \frac{z^2}{b^2} = 1$ $R_1 = \frac{a^2 b^2}{(a^2 \sin^2 \varphi + b^2 \cos^2 \varphi)^{3/2}}$ $R_2 = \frac{a^2}{(a^2 \sin^2 \varphi + b^2 \cos^2 \varphi)^{1/2}}$ $\varphi = \tan^{-1} \left( -\frac{b}{a} \sqrt{\frac{b^2}{z^2} - 1} \right)$
	<p><b><u>Cycloidal shell</u></b></p> $r = a (\psi + \sin \psi),$ $z = a (1 + \cos \psi)$ <p>where <math>-\pi \leq \psi \leq \pi</math></p> $R_1 = 2a \sqrt{2 + 2 \cos \psi}$ $R_2 = 2a \left( \frac{\psi}{2 \sin \psi} + \frac{1}{2} \right) \sqrt{2 + 2 \cos \psi}$ $\varphi = \tan^{-1} \left( \frac{-\sin \psi}{1 + \cos \psi} \right)$

Continue Table 1.1 Types of shells of revolution

Shell Geometry	Parameters
	<p><b><u>Parabolic shell</u></b></p> $z = b \left( 1 - \frac{r^2}{a^2} \right)$ $R_1 = \frac{a^2}{2b \cos^3 \phi} = \frac{a^2}{2b} \sec^3 \phi$ $R_2 = \frac{a^2}{2b \cos \phi} = \frac{a^2}{2b} \sec \phi$ $\phi = \tan^{-1} \left( \frac{-2b}{a^2} r \right)$
	<p><b><u>Hyperbolic shell</u></b></p> $\frac{r^2}{a^2} - \frac{z^2}{b^2} = 1$ $R_1 = \frac{a^2 b^2}{(a^2 \sin^2 \phi + b^2 \cos^2 \phi)^{3/2}}$ $R_2 = \frac{a^2}{(a^2 \sin^2 \phi + b^2 \cos^2 \phi)^{1/2}}$ $\phi = \tan^{-1} \left( \frac{r}{z} \tan^2 \psi \right) = \tan^{-1} \left( \frac{b^2}{a^2} \frac{r}{z} \right)$ $\psi = \tan^{-1}(b/a)$

### 1.3 Analytical solution of circular cylindrical shells

#### 1.3.1 Introduction

Analyzing the circular cylindrical shells has been considered by several authors by analytical solutions. We should mention that *Flügge* (1932) derived the governing differential equations for circular cylindrical shells in terms of displacements. Equations of the general theory of cylindrical shells were introduced by *Donnel* (1976). The analysis of circular cylindrical shells with uniform wall thickness is used in this study to verify the proposed mathematical model for analyzing water tanks.

The analysis of circular cylindrical shells with uniform wall thickness can be considered as indicated in the next paragraphs according to the references of *Timoshenko/ Woinowsky* (1959), *Bakhoun* (1992) and *Ventsel/ Krauthammer* (2001).

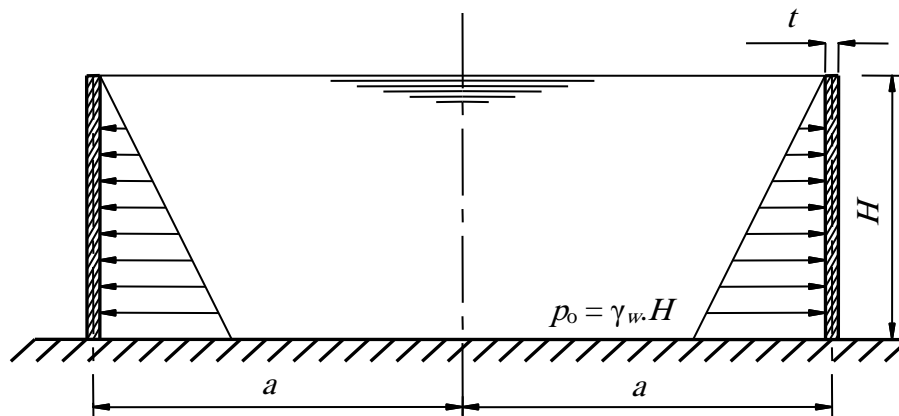


Figure 1.6 Cylindrical tank with uniform wall thickness

#### 1.3.2 General equation of circular cylindrical shell

To formulate the essential equation for determining the internal forces in a circular cylindrical shells with uniform wall thickness, consider the water tank in Figure 1.6 is submitted to the action of a water pressure. The water pressure  $p_x$  [kN/m<sup>2</sup>] in the wall at any position  $x$  [m] from the base can be obtained from:

$$p_x = p_o \frac{(H - x)}{H} \quad (4.8)$$

where:

$p_o$  Pressure at the wall base,  $p_o = \gamma_w \cdot H$ , [kN/m<sup>2</sup>]

$\gamma_w$  Unite weight of the water, [kN/m<sup>3</sup>]

$H$  Height of the tank, [m]

From the theory of elasticity, the differential equation for  $w$  can be obtained:

$$\frac{d^2}{dx^2} \left( D \frac{d^2 w}{dx^2} \right) + \frac{E t w}{a^2} = p_x \quad (4.9)$$

where:

$D$	Flexural rigidity (equation (4.3)).
$w$	Horizontal deflection along the $r$ axis at any point at distance $x$ from the base, [m]
$E$	<i>Young's</i> modulus of wall material, [kN/m <sup>2</sup> ]
$t$	Wall thickness, [m]
$a$	Tank radius, [m]

For a constant rigidity  $D$ , the above equation (4.9) may be written in the form:

$$\frac{d^4 w}{dx^4} + 4\beta^4 w = \frac{p_x}{D} \quad (4.10)$$

where  $\beta$  is a geometric parameter of the dimension [m<sup>-1</sup>] and equal:

$$\beta = \sqrt[4]{\frac{3(1 - \nu^2)}{a^2 t^2}} \quad (4.11)$$

A particular solution of the differential equation (4.10) is:

$$w_p = \frac{p_x a^2}{E t} \quad (4.12)$$

This expression represents the tangential expansion of a cylindrical shell with free edges under the action of hoop stresses. The general solution of equation (4.10) may be written in the form:

$$w = e^{\beta x}(C_1 \cos \beta x + C_2 \sin \beta x) + e^{-\beta x}(C_3 \cos \beta x + C_4 \sin \beta x) + \frac{p_x a^2}{E t} \quad (4.13)$$

where  $C_1$ ,  $C_2$ ,  $C_3$  and  $C_4$  are constants.

### 1.3.3 Boundary conditions

In most practical cases the wall thickness  $t$  is small in comparison with both the radius  $a$  and the height  $H$  of the tank. Therefore, the shell may be considered as infinitely long. Then, constants  $C_1$  and  $C_2$  are taken equal to zero, and this gives that:

$$w = e^{-\beta x}(C_3 \cos \beta x + C_4 \sin \beta x) + \frac{p_x a^2}{E t} \quad (4.14)$$

## Mathematical model

---

The constants  $C_3$  and  $C_4$  can now be obtained from the boundary conditions at the bottom of the tank. Assuming that the lower edge of the wall is built into an absolutely rigid foundation, the boundary conditions at  $x = 0$ , the deflection  $(w)_{x=0} = 0$ , then:

$$(w)_{x=0} = C_3 + \frac{p_x a^2}{Et} = 0 \quad (4.15)$$

and at  $x = 0$ , the rotation in tangential direction  $(\chi_s)_{x=0} = 0$ , then:

$$(\chi_s)_{x=0} = \left( \frac{dw}{dx} \right)_{x=0} = \left[ -\beta C_3 e^{-\beta x} (\cos \beta x + \sin \beta x) + \beta C_4 e^{-\beta x} (\cos \beta x - \sin \beta x) - \frac{p_o a^2}{EtH} \right]_{x=0} \quad (4.16)$$

$$(\chi_s)_{x=0} = \beta (C_4 - C_3) - \frac{p_o a^2}{EtH} = 0 \quad (4.17)$$

$$\chi_s = \beta e^{-\beta x} \left[ (C_4 - C_3) \cos \beta x - (C_4 + C_3) \sin \beta x \right] - \frac{p_o a^2}{EtH} \quad (4.18)$$

From these equations it's obtained that:

$$C_3 = A_1 = -\frac{p_o a^2}{Et} \quad C_4 = A_2 = \frac{p_o a^2}{Et} \left( \frac{1}{\beta H} - 1 \right) \quad (4.19)$$

### 1.3.4 Internal forces

The tangential force  $N_\theta$  in the circumferential direction is given by:

$$N_\theta = \frac{Et}{a} e^{-\beta x} (A_1 \cos \beta x + A_2 \sin \beta x) + p_x a \quad (4.20)$$

The tangential force  $N_s$  in the meridional direction or in the direction of the cylindrical shell axis is to be taken zero. From the second derivative of equation (4.14) the tangential bending moments  $M_s$  in the meridional direction is given by:

$$M_s = D \frac{d^2 w}{dx^2} = 2\beta^2 D e^{-\beta x} (A_1 \sin \beta x - A_2 \cos \beta x) \quad (4.21)$$

The tangential bending moments in the circumferential direction  $M_\theta$  is:

$$M_\theta = \nu D \frac{d^2 w}{dx^2} = \nu M_s \quad (4.22)$$

The transverse shearing force  $Q_s$  of a section perpendicular to the axis of a cylindrical shell is given by:

$$Q_s = -D \frac{d^3 w}{dx^3} = -2\beta^3 D e^{-\beta x} [(A_2 + A_1) \cos \beta x + (A_2 - A_1) \sin \beta x] \quad (4.23)$$

## 1.4 Finite elements analysis of axi-symmetric shells of revolution

### 1.4.1 Introduction

Circular cylindrical shells analysis may be considered as an axi-symmetric shell structure problem. An axi-symmetric shell structure can be idealized by a series of conical frustum-shaped elements as shown in Figure 1.7. This element was first suggested by *Grafton and Strome* (1963) and later its use was extended by *Percy et al* (1965). It may be noted that this single element has two ring nodes. Since both in-plan and out of plan displacements and forces have to be considered in shell structures, the displacement vector for each node contains axial and radial movements as well as rotation as shown in Figure 1.7 - b). Finite element analysis of axi-symmetric shells in the simplified approach of *Grafton and Strome* (1963) are presented by many authors. Some of them are *Zienkiewicz/ Cheung* (1967), *Rockey et al* (1975), *Szilard* (1986), and *Melerski* (2000). *Szilard* (1986) presented a more extensive analysis of axi-symmetric shell structure with a computer program code. The following steps of the FE analysis of axi-symmetric shell structure depends on that of *Zienkiewicz/ Cheung* (1967) and *Rockey et al* (1975).

### 1.4.2 Nodal vectors of displacements and forces

It is convenient to use cylindrical polar co-ordinates  $(r, z)$  and considering node (1) in Figure 1.7. The nodal displacement vector is written as:

$$\{\delta_1\} = \begin{Bmatrix} \bar{u}_1 \\ \bar{w}_1 \\ \chi_{s1} \end{Bmatrix} \quad (4.24)$$

where:

- $\bar{u}$  Axial displacement in global co-ordinates, [-]
- $\bar{w}$  Horizontal radial displacement in global co-ordinates, [-]
- $\chi_s$  Meridional rotation, [Rad].

The corresponding forces at node (1) are:

$$\{F_1\} = \begin{Bmatrix} F_{z1} \\ F_{r1} \\ M_1 \end{Bmatrix} \quad (4.25)$$

where:

- $F_z$  Axial force in global co-ordinates, [kN/m]
- $F_r$  Radial force in global co-ordinates, [kN/m]
- $M$  Meridional bending moment, [kN.m/m].

## Mathematical model

---

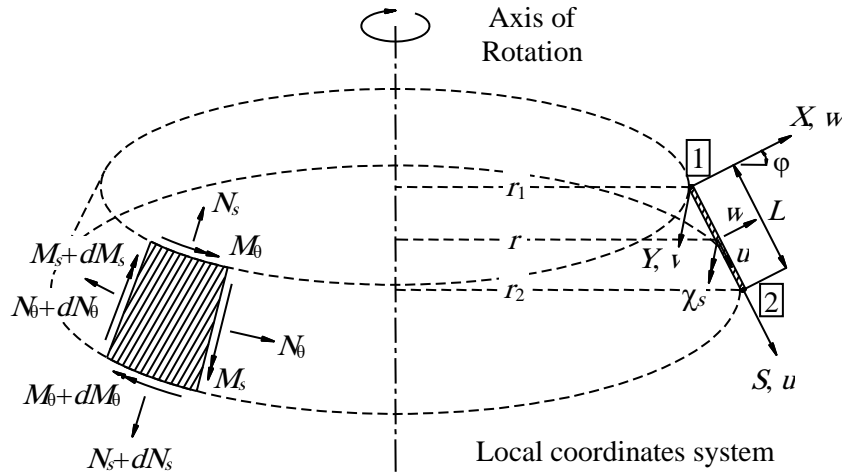
The complete displacement and force vectors for the element, i.e. nodes (1) and (2), may be written as:

$$\{\delta^e\} = \begin{Bmatrix} \{\delta_1\} \\ \{\delta_2\} \end{Bmatrix} = \begin{Bmatrix} \bar{u}_1 \\ \bar{w}_1 \\ \chi_{s1} \\ \bar{u}_2 \\ \bar{w}_2 \\ \chi_{s2} \end{Bmatrix} \quad (4.26)$$

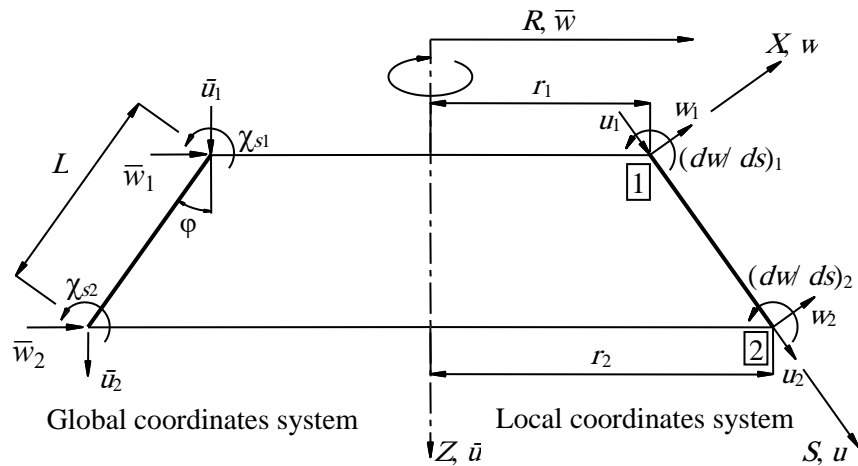
$$\{F^e\} = \begin{Bmatrix} \{F_1\} \\ \{F_2\} \end{Bmatrix} = \begin{Bmatrix} F_{z1} \\ F_{r1} \\ M_1 \\ F_{z2} \\ F_{r2} \\ M_2 \end{Bmatrix} \quad (4.27)$$

Thus each axi-symmetric shell element has six degrees of freedom and the complete element stiffness matrix  $[K^e]$  is of size  $6 \times 6$ .

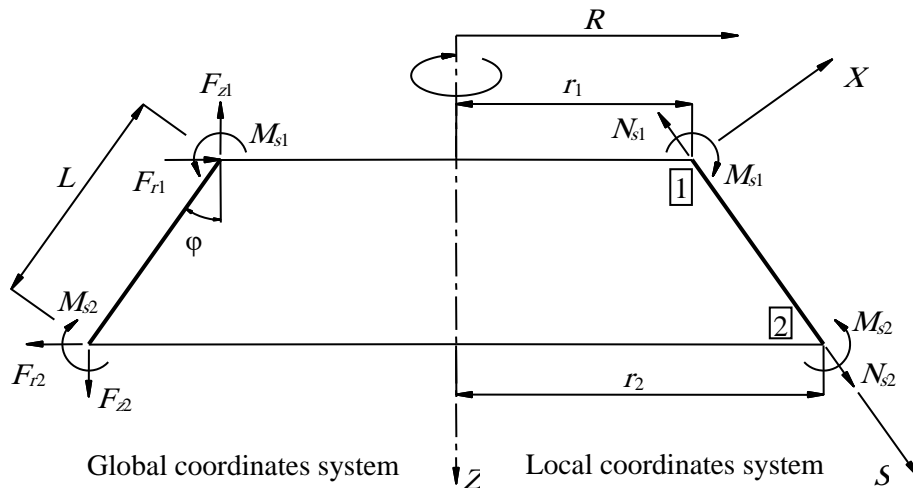
$$\{F^e\} = [K^e]\{\delta^e\} \quad (4.28)$$



a) Internal forces for conical shell element



b) Deformations at the nodes in the local (right) and global (left) coordinate systems



c) Forces at the nodes in the local (right) and global (left) coordinate systems

Figure 1.7 Conical ring shell element

### 1.4.3 Displacement function

Because of the inclination of the element  $\varphi$  to the  $z$ -axis of the shell, it is more convenient to specify the element displacement function in terms of local element co-ordinates  $(r, s)$ , where  $u$  is the in-plan (tangential) displacement and  $w$  is the displacement normal to the plan as shown in Figure 1.7. Since there are six degrees of freedom per element, six unknown coefficients have to be taken in the polynomials representing the permitted displacement pattern. Equation (4.29) gives a suitable set of relationships in which the in-plan displacement function  $u$  varies linearly in  $s$  and  $w$  varies as a cubic in  $s$ .

$$\left. \begin{aligned} u &= \alpha_1 + \alpha_2 s \\ w &= \alpha_3 + \alpha_4 s + \alpha_5 s^2 + \alpha_6 s^3 \\ \frac{dw}{ds} &= \alpha_4 + 2\alpha_5 s + 3\alpha_6 s^2 \end{aligned} \right\} \quad (4.29)$$

where:

$\alpha_{1, 2, \dots, 6}$	Constants used in displacement function, [-].
$u$	Meridional displacement in local co-ordinates, [cm].
$w$	Normal displacement in local co-ordinates, [cm].
$dw/ds$	Meridional rotation, [Rad].

It may be noted that the third equation for the rotation  $dw/ds$  is obtained by differentiating the second. Writing equation (4.29) in matrix form, the relationship in equation (4.30) between the element displacements  $u$  and  $w$  and the undetermined coefficient  $\alpha$  is obtained.

$$\begin{Bmatrix} u \\ w \\ \frac{dw}{ds} \end{Bmatrix} = \begin{bmatrix} 1 & s & 0 & 0 & 0 & 0 \\ 0 & 0 & 1 & s & s^2 & s^3 \\ 0 & 0 & 0 & 1 & 2s & 3s^2 \end{bmatrix} \begin{Bmatrix} \alpha_1 \\ \alpha_2 \\ \alpha_3 \\ \alpha_4 \\ \alpha_5 \\ \alpha_6 \end{Bmatrix} \quad (4.30)$$

Equation (4.30) may be written in matrix form as:

$$\{\delta(r, s)\} = [f(r, s)]\{\alpha\} \quad (4.31)$$

where:

$f(r, s)$	Matrix of displacement function.
$\delta(r, s)$	Nodal displacement vector in local co-ordinate system.
$\{\alpha\}$	Vector of displacement coefficients.

#### 1.4.4 Displacement transformation from local to global co-ordinates

The constants  $\alpha_1$  to  $\alpha_6$  can be evaluated by writing down the six simultaneous equations concerning the values of the nodal co-ordinates ( $r, s$ ). Listing all six equations and substituting the node coordinate by element dimension  $L$  yields to a relationship for the constants  $\{\alpha\}$ :

$$\begin{Bmatrix} u_1 \\ w_1 \\ \left(\frac{dw}{ds}\right)_1 \\ u_2 \\ w_2 \\ \left(\frac{dw}{ds}\right)_2 \end{Bmatrix} = \begin{bmatrix} 1 & 0 & 0 & 0 & 0 & 0 \\ 0 & 0 & 1 & 0 & 0 & 0 \\ 0 & 0 & 0 & 1 & 0 & 0 \\ 1 & L & 0 & 0 & 0 & 0 \\ 0 & 0 & 1 & L & L^2 & L^3 \\ 0 & 0 & 0 & 1 & 2L & 3L^2 \end{bmatrix} \begin{Bmatrix} \alpha_1 \\ \alpha_2 \\ \alpha_3 \\ \alpha_4 \\ \alpha_5 \\ \alpha_6 \end{Bmatrix} \quad (4.32)$$

Inverting equation (4.32) gives:

$$\begin{Bmatrix} \alpha_1 \\ \alpha_2 \\ \alpha_3 \\ \alpha_4 \\ \alpha_5 \\ \alpha_6 \end{Bmatrix} = \begin{bmatrix} 1 & 0 & 0 & 0 & 0 & 0 \\ -\frac{1}{L} & 0 & 0 & \frac{1}{L} & 0 & 0 \\ 0 & 1 & 0 & 0 & 0 & 0 \\ 0 & 0 & 1 & 0 & 0 & 0 \\ 0 & -\frac{3}{L^2} & -\frac{2}{L} & 0 & \frac{3}{L^2} & -\frac{1}{L} \\ 0 & \frac{2}{L^3} & \frac{1}{L^2} & 0 & -\frac{2}{L^3} & \frac{1}{L^2} \end{bmatrix} \begin{Bmatrix} u_1 \\ w_1 \\ \left(\frac{dw}{ds}\right)_1 \\ u_2 \\ w_2 \\ \left(\frac{dw}{ds}\right)_2 \end{Bmatrix} \quad (4.33)$$

Therefore, using equations (4.30) and (4.33), one gets the displacements  $\{u, w\}$  at any point within the element are expressed in terms of the displacements at nodes 1 and 2, as:

$$\begin{Bmatrix} u \\ w \end{Bmatrix} = \begin{bmatrix} 1-p & 0 & 0 & p & 0 & 0 \\ 0 & 1-3p^2+2p^3 & Lp-2Lp^2+Lp^3 & 0 & 3p^2-2p^3 & -Lp^2+Lp^3 \end{bmatrix} \begin{Bmatrix} u_1 \\ w_1 \\ \left(\frac{dw}{ds}\right)_1 \\ u_2 \\ w_2 \\ \left(\frac{dw}{ds}\right)_2 \end{Bmatrix} \quad (4.34)$$

where  $p = s/L$

Referring to equation (4.34) it is seen that:

$$\left. \begin{aligned} u_1 &= \bar{u}_1 \cos \varphi + \bar{w}_1 \sin \varphi \\ w_1 &= -\bar{u}_1 \sin \varphi + \bar{w}_1 \cos \varphi \\ \left(\frac{dw}{ds}\right)_1 &= \chi_{s1} \end{aligned} \right\} \quad (4.35)$$

Writing these equations in matrix form the transformation matrix for node (1) is:

$$\left\{ \begin{array}{c} u_1 \\ w_1 \\ \left(\frac{dw}{ds}\right)_1 \end{array} \right\} = \begin{bmatrix} \cos\varphi & \sin\varphi & 0 \\ -\sin\varphi & \cos\varphi & 0 \\ 0 & 0 & 1 \end{bmatrix} \left\{ \begin{array}{c} \bar{u}_1 \\ \bar{w}_1 \\ \chi_{s1} \end{array} \right\} = [T]\{\delta_1\} \quad (4.36)$$

For a single element,

$$\left\{ \begin{array}{c} u_1 \\ w_1 \\ \left(\frac{dw}{ds}\right)_1 \\ u_2 \\ w_2 \\ \left(\frac{dw}{ds}\right)_2 \end{array} \right\} = \begin{bmatrix} \cos\varphi & \sin\varphi & 0 & 0 & 0 & 0 \\ -\sin\varphi & \cos\varphi & 0 & 0 & 0 & 0 \\ 0 & 0 & 1 & 0 & 0 & 0 \\ 0 & 0 & 0 & \cos\varphi & \sin\varphi & 0 \\ 0 & 0 & 0 & -\sin\varphi & \cos\varphi & 0 \\ 0 & 0 & 0 & 0 & 0 & 1 \end{bmatrix} \left\{ \begin{array}{c} \bar{u}_1 \\ \bar{w}_1 \\ \chi_{s1} \\ \bar{u}_2 \\ \bar{w}_2 \\ \chi_{s2} \end{array} \right\} \quad (4.37)$$

Therefore, substituting from equation (4.37) in equation (4.34), equation (4.34) can be written in the form:

$$\left\{ \begin{array}{c} u \\ w \end{array} \right\} = \begin{bmatrix} (1-p)\cos\varphi & (1-p)\sin\varphi & 0 \\ -(1-3p^2+2p^3)\sin\varphi & (1-3p^2+2p^3)\cos\varphi & L(p-2p^2+p^3) \\ p\cos\varphi & p\sin\varphi & 0 \\ -(3p^2-2p^3)\sin\varphi & (3p^2-2p^3)\cos\varphi & L(-p^2+p^3) \end{bmatrix} \left\{ \begin{array}{c} \bar{u}_1 \\ \bar{w}_1 \\ \chi_{s1} \\ \bar{u}_2 \\ \bar{w}_2 \\ \chi_{s2} \end{array} \right\} \quad (4.38)$$

### 1.4.5 Strain-displacement formulation

The components of strain for the middle surface of a conical frustum axi-symmetric shell involve extensions and curvatures which are the two in-plan strains  $\varepsilon_s$  and  $\varepsilon_\theta$  (hoop strain), and the corresponding curvatures  $\kappa_s$  and  $\kappa_\theta$ . These are related to the displacements  $u$  and  $w$  by equation (4.39).

$$\{\varepsilon(r, s)\} = \begin{Bmatrix} \varepsilon_s \\ \varepsilon_\theta \\ \kappa_s \\ \kappa_\theta \end{Bmatrix} = \begin{bmatrix} \frac{d}{ds} & 0 \\ \frac{\sin\varphi}{r} & \frac{\cos\varphi}{r} \\ 0 & \frac{-d^2}{ds^2} \\ 0 & \frac{-\sin\varphi}{r} \frac{d}{ds} \end{bmatrix} \begin{Bmatrix} u \\ w \end{Bmatrix} \quad (4.39)$$

It should be noted that since  $p = s/L$ ,  $ds = L dp$  and  $\frac{d}{ds} = \frac{1}{L} \frac{d}{dp}$

Substituting from equation (4.38) and performing the differentiations indicated in equation (4.39) gives the strain-nodal displacement matrix  $[B]$ :

$$\{\varepsilon(r, s)\} = [B] \{\delta^e\} \quad (4.40)$$

in which:

$$[B] = \begin{bmatrix} \frac{-\cos\varphi}{L} & \frac{-\sin\varphi}{L} & 0 \\ (1-p) \frac{\sin 2\varphi}{2r} - (1-3p^2+2p^3) \frac{\sin 2\varphi}{2r} & (1-p) \frac{\sin^2\varphi}{r} + (1-3p^2+2p^3) \frac{\cos^2\varphi}{r} & (p-2p^2+p^3) \frac{L\cos\varphi}{r} \\ -(-6+12p) \frac{\sin\varphi}{L^2} & (-6+12p) \frac{\cos\varphi}{L^2} & -(-4+6p) \frac{1}{L} \\ (-6p+6p^2) \frac{\sin^2\varphi}{rL} & -(-6p+6p^2) \frac{\sin 2\varphi}{2rL} & -(1-4p+3p^2) \frac{\sin\varphi}{r} \end{bmatrix} \quad (4.41)$$

$$\begin{bmatrix} \frac{\cos\varphi}{L} & \frac{\sin\varphi}{L} & 0 \\ p \frac{\sin 2\varphi}{2r} - (3p^2-2p^3) \frac{\sin 2\varphi}{2r} & p \frac{\sin^2\varphi}{r} + (3p^2-2p^3) \frac{\cos^2\varphi}{r} & (-p^2+p^3) \frac{L\cos\varphi}{r} \\ (-6+12p) \frac{\sin\varphi}{L^2} & -(-6+12p) \frac{\cos\varphi}{L^2} & -(-2+6p) \frac{1}{L} \\ -(-6p+6p^2) \frac{\sin^2\varphi}{rL} & (-6p+6p^2) \frac{\sin 2\varphi}{2rL} & -(-2p+3p^2) \frac{\sin\varphi}{r} \end{bmatrix}$$

and the transposed matrix  $[B]^T$  is:

$$[B]^T = \begin{bmatrix} \frac{-\cos\varphi}{L} & (1-p)\frac{\sin 2\varphi}{2r} - (1-3p^2+2p^3)\frac{\sin 2\varphi}{2r} & -(-6+12p)\frac{\sin\varphi}{L^2} & (-6p+6p^2)\frac{\sin^2\varphi}{rL} \\ \frac{-\sin\varphi}{L} & (1-p)\frac{\sin^2\varphi}{r} + (1-3p^2+2p^3)\frac{\cos^2\varphi}{r} & (-6+12p)\frac{\cos\varphi}{L^2} & -(-6p+6p^2)\frac{\sin 2\varphi}{2rL} \\ 0 & (p-2p^2+p^3)\frac{L\cos\varphi}{r} & -(-4+6p)\frac{1}{L} & -(1-4p+3p^2)\frac{\sin\varphi}{r} \\ \frac{\cos\varphi}{L} & p\frac{\sin 2\varphi}{2r} - (3p^2-2p^3)\frac{\sin 2\varphi}{2r} & (-6+12p)\frac{\sin\varphi}{L^2} & -(-6p+6p^2)\frac{\sin^2\varphi}{rL} \\ \frac{\sin\varphi}{L} & p\frac{\sin^2\varphi}{r} + (3p^2-2p^3)\frac{\cos^2\varphi}{r} & -(-6+12p)\frac{\cos\varphi}{L^2} & (-6p+6p^2)\frac{\sin 2\varphi}{2rL} \\ 0 & (-p^2+p^3)\frac{L\cos\varphi}{r} & -(-2+6p)\frac{1}{L} & -(-2p+3p^2)\frac{\sin\varphi}{r} \end{bmatrix} \quad (4.42)$$

To calculate the matrix  $[B]$  for nodes 1 and 2, by substituting  $p = 0$ ,  $r = r_1$  for node 1 and  $p = 1$ ,  $r = r_2$  for node 2:

$$[B_1] = \begin{bmatrix} \frac{-\cos\varphi}{L} & \frac{-\sin\varphi}{L} & 0 & \frac{\cos\varphi}{L} & \frac{\sin\varphi}{L} & 0 \\ 0 & \frac{1}{r_1} & 0 & 0 & 0 & 0 \\ \frac{6\sin\varphi}{L^2} & \frac{-6\cos\varphi}{L^2} & \frac{4}{L} & \frac{-6\sin\varphi}{L^2} & \frac{6\cos\varphi}{L^2} & \frac{2}{L} \\ 0 & 0 & \frac{-\sin\varphi}{r_1} & 0 & 0 & 0 \end{bmatrix}$$

$$[B_2] = \begin{bmatrix} \frac{-\cos\varphi}{L} & \frac{-\sin\varphi}{L} & 0 & \frac{\cos\varphi}{L} & \frac{\sin\varphi}{L} & 0 \\ 0 & 0 & 0 & 0 & \frac{1}{r_2} & 0 \\ \frac{-6\sin\varphi}{L^2} & \frac{6\cos\varphi}{L^2} & \frac{-2}{L} & \frac{-6\sin\varphi}{L^2} & \frac{-6\cos\varphi}{L^2} & \frac{-4}{L} \\ 0 & 0 & 0 & 0 & 0 & \frac{-\sin\varphi}{r_2} \end{bmatrix} \quad (4.43)$$

### 1.4.6 Stress-displacement formulation

In the case of shells, it is usual to work in terms of the stress resultants, which are the forces and moments per unit length. For this axi-symmetric shell element these resultants consists of  $N_s, N_\theta$  which are the membrane forces per unit length, and  $M_s, M_\theta$ , the moments per unit length, as shown in Figure 1.7. The stress-strain matrix,  $[D]$  is given by:

$$\{\sigma(r, s)\} = \begin{Bmatrix} N_s \\ N_\theta \\ M_s \\ M_\theta \end{Bmatrix} = \frac{Et}{(1-\nu^2)} \begin{bmatrix} 1 & \nu & 0 & 0 \\ \nu & 1 & 0 & 0 \\ 0 & 0 & \frac{t^2}{12} & \frac{\nu t^2}{12} \\ 0 & 0 & \frac{\nu t^2}{12} & \frac{t^2}{12} \end{bmatrix} \begin{Bmatrix} \varepsilon_s \\ \varepsilon_\theta \\ \kappa_s \\ \kappa_\theta \end{Bmatrix} \quad (4.44)$$

The above equation may be written in compacted matrix form as  $\{\sigma(r, s)\} = [D] \{\varepsilon(r, s)\}$

where:

- $E$  Young's modulus of elasticity, [kN/m<sup>2</sup>]
- $\nu$  Poisson's ratio, [-]
- $t$  Shell thickness, [m]

Substituting from equations (4.40) and (4.41) into equation (4.44) yields the stresses in the element related to the nodal displacements:

$$\{\sigma(r, s)\} = [D][B]\{\delta^e\} = [H]\{\delta^e\} \quad (4.45)$$

The stress-displacement matrix  $[H]$  is obtained by pre-multiplying the matrix  $[B]$  given in equation (4.41) by the  $[D]$  matrix given in equation (4.44), where, for nodes 1 and 2

$$[D]_{8 \times 8} = \begin{bmatrix} D_1 & 0 \\ 0 & D_2 \end{bmatrix} \text{ and } [B]_{8 \times 6} = \begin{bmatrix} B_1 \\ B_2 \end{bmatrix} \quad (4.46)$$

$$[H] = \frac{Et}{(1-\nu^2)} \begin{bmatrix} \frac{-\cos\varphi}{L} & \frac{\nu}{r_1} - \frac{\sin\varphi}{L} & 0 & \frac{\cos\varphi}{L} & \frac{\sin\varphi}{L} & 0 \\ \frac{-\nu\cos\varphi}{L} & \frac{1}{r_1} - \frac{\nu\sin\varphi}{L} & 0 & \frac{\nu\cos\varphi}{L} & \frac{\nu\sin\varphi}{L} & 0 \\ \frac{t^2\sin\varphi}{2L^2} & \frac{-t^2\cos\varphi}{2L^2} & \frac{t^2}{3L} - \frac{\nu t^2\sin\varphi}{12r_1} & \frac{-t^2\sin\varphi}{2L^2} & \frac{t^2\cos\varphi}{2L^2} & \frac{-t^2}{6L} \\ \frac{\nu t^2\sin\varphi}{2L^2} & \frac{-\nu t^2\cos\varphi}{2L^2} & \frac{\nu t^2}{3L} - \frac{t^2\sin\varphi}{12r_1} & \frac{-\nu t^2\sin\varphi}{2L^2} & \frac{\nu t^2\cos\varphi}{2L^2} & \frac{-\nu t^2}{6L} \\ \frac{-\cos\varphi}{L} & \frac{\sin\varphi}{L} & 0 & \frac{\cos\varphi}{L} & \frac{\nu}{r_2} + \frac{\sin\varphi}{L} & 0 \\ \frac{-\nu\cos\varphi}{L} & \frac{\nu\sin\varphi}{L} & 0 & \frac{\nu\cos\varphi}{L} & \frac{1}{r_2} + \frac{\nu\sin\varphi}{L} & 0 \\ \frac{-t^2\sin\varphi}{2L^2} & \frac{t^2\cos\varphi}{2L^2} & \frac{t^2}{6L} & \frac{t^2\sin\varphi}{2L^2} & \frac{-t^2\cos\varphi}{2L^2} & \frac{t^2}{3L} - \frac{\nu t^2\sin\varphi}{12r_2} \\ \frac{-\nu t^2\sin\varphi}{2L^2} & \frac{\nu t^2\cos\varphi}{2L^2} & \frac{\nu t^2}{6L} & \frac{\nu t^2\sin\varphi}{2L^2} & \frac{-\nu t^2\cos\varphi}{2L^2} & \frac{\nu t^2}{3L} - \frac{t^2\sin\varphi}{12r_2} \end{bmatrix} \quad (4.47)$$

#### 1.4.7 Stiffness matrix formulation

The internal stresses  $\{\sigma(r, s)\}$  are now replaced by statically equivalent nodal loads  $\{F^e\}$  and hence the nodal loads are related to the nodal displacements  $\{\delta^e\}$  thereby defining the required element stiffness matrix  $[K^e]$ . The principle of virtual work is used to determine the set of nodal loads that is statically equivalent to the internal stresses. The condition of equivalence may be expressed as follows: during any virtual displacement imposed on the element, the total external work done by the nodal loads must equal the total internal work done by the stresses. An arbitrary set of nodal displacements represented by the vector  $\{\delta^{*e}\}$  is selected where:

$$\{\delta^{*e}\} = \begin{Bmatrix} \{\delta_1^{*e}\} \\ \{\delta_2^{*e}\} \\ \vdots \\ \{\delta_n^{*e}\} \end{Bmatrix} \quad (4.48)$$

The external work done by the nodal loads  $W_{ext}$  is given by:

$$W_{ext} = \{\delta_1^{*e}\}\{F_1^e\} + \{\delta_2^{*e}\}\{F_2^e\} + \dots + \{\delta_n^{*e}\}\{F_n^e\} = \{\delta^{*e}\}\{F^e\} \quad (4.49)$$

If the arbitrarily imposed displacements cause strains  $\{\varepsilon(r, s)^*\}$  at a point within the element where the actual stress are  $\{\sigma(r, s)\}$ , then the internal work done per unit volume is given by:

$$W_{int} = \{\varepsilon(r, s)^*\}^T \{\sigma(r, s)\} \quad (4.50)$$

And the total internal work is obtained by integrating over the volume of the element, namely:

$$\int^V W_{int} d(\text{vol}) = \int^V \{\varepsilon(r, s)\}^T \{\sigma(r, s)\} d(\text{vol}) \quad (4.51)$$

Now from equation (4.40) it is known that the strains set up at any point in the element are given in terms of the nodal displacements by  $\{\varepsilon(r, s)\} = [B]\{\delta^e\}$ . Hence when nodal displacements  $\{\delta^{*e}\}$  are imposed, the corresponding strains may be written as  $\{\varepsilon(r, s)\} = [B]\{\delta^{*e}\}$ .

Furthermore, from equation (4.45) the actual stresses in the element are known to be related to the actual nodal displacements. Therefore, these expressions may be substituted into the virtual work equation for the internal work to obtain:

$$\int^V W_{int} d(\text{vol}) = \int^V [B]^T \{\delta^{*e}\} [D][B] \{\delta^e\} d(\text{vol}) \quad (4.52)$$

and

$$W_{ext} = \{\delta^{*e}\}^T \{F^e\} \quad (4.53)$$

The final operation is to equate internal and external work done during the system of virtual displacements  $\{\delta^{*e}\}$ . Since the basic principle of virtual displacements is valid for any system of applied displacements the selection of the system of virtual nodal displacements may be chosen at will. For present purposes, it is convenient to assume that the unit values of the nodal displacements are applied. Then equating the internal and external work gives:

$$\{F^e\} = \left[ \int^V [B]^T [D][B] d(\text{vol}) \right] \{\delta^e\} \quad (4.54)$$

on comparing equation (4.54) with equation (4.55), which is stated below:

$$\{F^e\} = [K^e] \{\delta^e\} \quad (4.55)$$

It is clear that the required element stiffness matrix  $[K^e]$  is given by the expression in the large square brackets in equation (4.56). Therefore:

$$[K^e] = \int^V [B]^T [D][B] d(\text{vol}) \quad (4.56)$$

and, for a constant small element thickness  $t$ , the element stiffness matrix is obtained by integrating over the area of the element, namely:

$$[K^e] = \int^A [B]^T [D][B] dA \quad (4.57)$$

where

$$dA = 2\pi r(s) ds = 2\pi L r(p) dp \quad (4.58)$$

$$r(s) = (r_2 - r_1/L) s + r_1 \quad (4.59)$$

$$r(p) = (r_2 - r_1) p + r_1 \quad (4.60)$$

with  $p$  varying from 0 to 1. Thus, the stiffness matrix becomes:

$$[K^e] = 2\pi L \int_0^1 [B]^T [D] [B] ((r_2 - r_1)p + r_1) dp \quad (4.61)$$

$$[K^e] = 2\pi L \int_0^1 [B]^T [H] ((r_2 - r_1)p + r_1) dp \quad (4.62)$$

where for nodes 1 and 2:

$$[B]^T_{6 \times 8} = \begin{bmatrix} B_1 \\ B_2 \end{bmatrix}^T, [D]_{8 \times 8} = \begin{bmatrix} D_1 & 0 \\ 0 & D_2 \end{bmatrix}, [B]_{8 \times 6} = \begin{bmatrix} B_1 \\ B_2 \end{bmatrix} \text{ and } [H]_{8 \times 6} = \begin{bmatrix} H_1 \\ H_2 \end{bmatrix} \quad (4.63)$$

According to *Szilard, Ziesing and Pickhardt* (1986), the elements of the (transformed) stiffness matrix for the general case of any angle  $\varphi$  is:

$$[K^e] = \begin{bmatrix} K_{11} & K_{12} & K_{13} & K_{14} & K_{15} & K_{16} \\ & K_{22} & K_{23} & K_{24} & K_{25} & K_{26} \\ & & K_{33} & K_{34} & K_{35} & K_{36} \\ & & & K_{44} & K_{45} & K_{46} \\ \text{Symm.} & & & & K_{55} & K_{56} \\ & & & & & K_{66} \end{bmatrix} \quad (4.64)$$

where:

$$K_{11} = \frac{\pi}{L} \left( \frac{12}{t^2} D(r_1+r_2) \cos^2 \varphi + \frac{36}{L^2} D(r_1+r_2) \sin^2 \varphi \right) = K_{14}$$

$$K_{12} = \frac{\pi}{L} \cos \varphi \left( \frac{12}{t^2} D(r_1+r_2) \sin \varphi - \frac{12}{t^2} DLv - \frac{36}{L^2} D(r_1+r_2) \sin \varphi \right)$$

$$K_{13} = -\frac{6\pi}{L^2} \sin \varphi (2D(2r_1+r_2) - DLv \sin \varphi)$$

$$K_{15} = -\frac{\pi}{L} \cos \varphi \left( \frac{12}{t^2} D(r_1+r_2) \sin \varphi + \frac{12}{t^2} DLv - \frac{36}{L^2} D(r_1+r_2) \sin \varphi \right)$$

$$K_{16} = -\frac{6\pi}{L^2} \sin \varphi (2D(r_1+2r_2) + DLv \sin \varphi)$$

$$K_{22} = \frac{\pi}{L} \left( \frac{12}{t^2} D(r_1+r_2) \sin^2 \varphi - \frac{24}{t^2} DLv \sin \varphi + \frac{12L^2}{r_1 t^2} D + \frac{36}{L^2} D(r_1+r_2) \cos^2 \varphi \right)$$

$$K_{23} = \frac{6\pi}{L^2} \cos\varphi (2D(2r_1+r_2) - DLv\sin\varphi); K_{24} = -K_{12}$$

$$K_{25} = -\frac{\pi}{L} \left( \frac{12}{t^2} D(r_1+r_2) \sin^2\varphi + \frac{36}{L^2} D(r_1+r_2) \cos^2\varphi \right)$$

$$K_{26} = \frac{6\pi}{L^2} \cos\varphi (2D(r_1+2r_2) + DLv\sin\varphi)$$

$$K_{33} = \frac{4\pi}{L} \left( D(4r_1+r_2) - 2DLv\sin\varphi + D \frac{L^2}{4r_1} \sin^2\varphi \right); K_{34} = -K_{15}; K_{35} = -K_{23}$$

$$K_{36} = \frac{2\pi}{L} (4D(r_1+r_2)); K_{44} = K_{11}; K_{45} = -K_{15}; K_{46} = -K_{16}$$

$$K_{55} = \frac{\pi}{L} \left( \frac{12}{t^2} D(r_1+r_2) \sin^2\varphi + \frac{24}{t^2} DLv\sin\varphi + \frac{12L^2}{r_2 t^2} D + \frac{36}{L^2} D(r_1+r_2) \cos^2\varphi \right)$$

$$K_{56} = -\frac{6\pi}{L^2} \cos\varphi (2D(r_1+2r_2) + DLv\sin\varphi)$$

$$K_{66} = \frac{\pi}{L} \left( 4D(r_1+4r_2) + 8DLv\sin\varphi + D \frac{L^2}{r_2} \sin^2\varphi \right)$$

Where  $D$  is the flexural rigidity as shown in Eq. (4.3)

#### 1.4.8 Calculation process with axially symmetrical loading

The calculation of axially symmetrical loaded shells of revolution is carried out in the usual way by the finite element method. The structure is converted into a quasi-one-dimensional replacement system using conical ring shell elements. The geometry of this replacement system is defined in a global reference system  $Z, R$  by the cylindrical coordinates of the nodes  $(z_i, r_i)$ . The  $Z$ -axis is selected as the axis of rotation. The origin of the coordinate system is usually set in the vertex of the axi-symmetric shell.

Next, the authorized global nodes deformations are numbered. The overall stiffness matrix of the structure  $K$  is carried out by superposition of the individual values of the stiffness indices.

$$K_{ij} = \sum_{ij} k'_{ij} \quad (4.65)$$

After assembling the overall stiffness matrix, the given boundary conditions should be incorporated. The outer surface loading must be converted into a resultant force acting on the nodes in the vertical or horizontal direction.

**1.4.9 Simulation of circular plate**

Equations (4.43), (4.64) and (4.47) present a conical element with any tangential angle  $\varphi$ . For circular cylindrical shells  $\varphi = 0$  [°], while for circular plates  $\varphi = 90$  [°].

Shells are often closed at the ends like conical shell elements or circular plates. Both cases can be treated with appropriate limits of the element dimensions. At cone vertex (Figure 1.8- a))  $r_1$  or  $r_2$  may not be exactly zero, because the values of the matrix elements in equation (4.65) become deteriorated, as  $r_1$  or  $r_2$  are divisors. To avoid unauthorized division by zero, *ELPLA* changes internally the entered zero value with a radius equal to  $10^{-3}$  [m]. Circular plates have to be analyzed also with a fictional small overall height (for example,  $10^{-3}$  [m]) (Figure 1.8 b)). Taking these limitations, wall of the circular cylindrical tank with circular base plate are analyzed using the same shell elements.

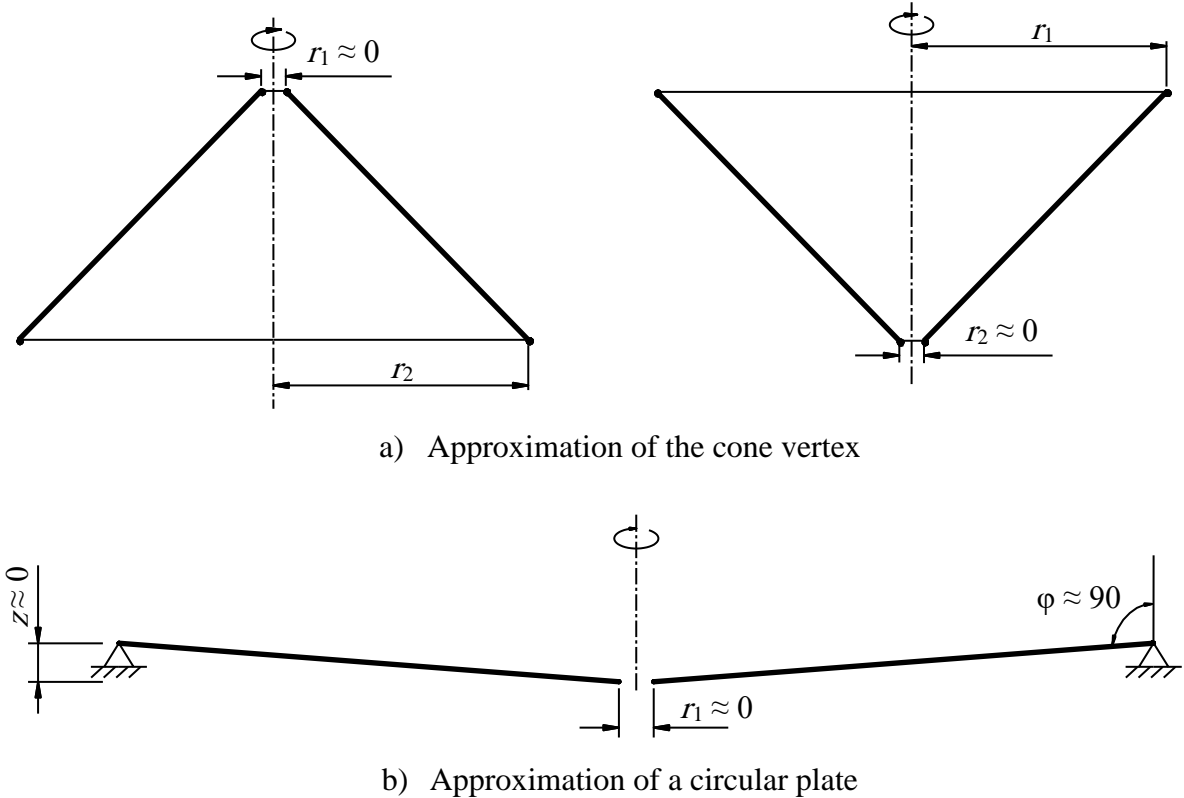


Figure 1.8 Boundary values for element dimensions

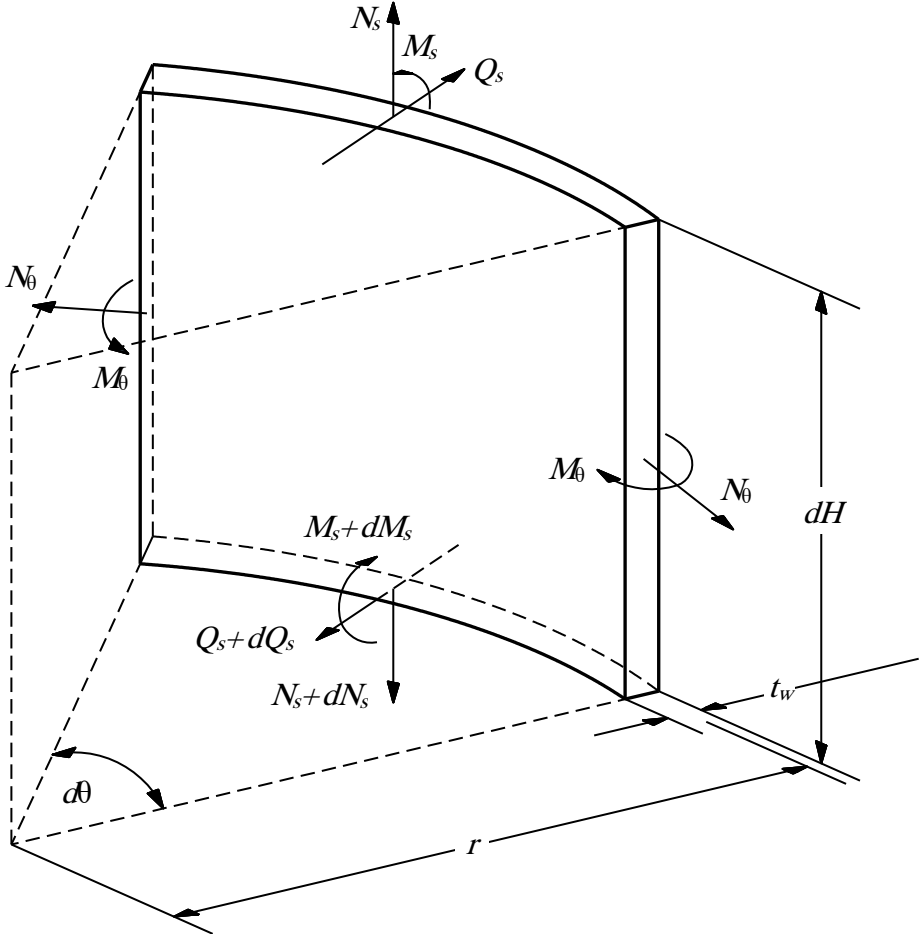
---

#### 1.4.10 Simulation of the tank wall and base using thin shell element

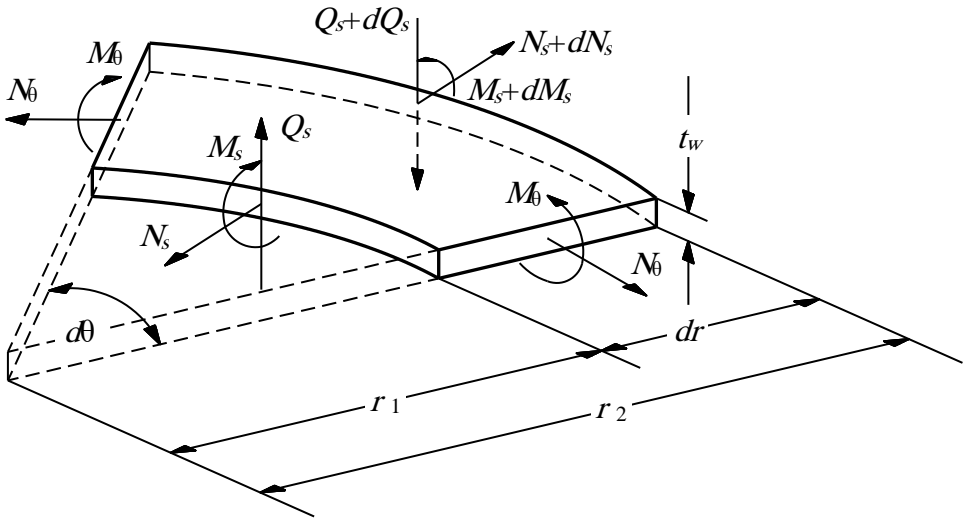
The analysis of the tanks used in this book are carried out numerically by *ELPLA*, where the circular cylindrical wall and the base were simulated with a thin shell element using finite element method.

Figure 1.9-a shows the internal forces acting on a cylindrical shell element which simulates the wall of the tank, while Figure 1.9-b shows the internal forces acting on a circular flat shell element which simulates the base of the tank.

Considering the two shell elements, the internal forces acting on these elements are the tangential normal force ( $N_\theta$ ), the meridional normal force ( $N_s$ ), the tangential bending moment ( $M_\theta$ ), the meridional bending moment ( $M_s$ ) and the transverse shearing force component ( $Q_s$ ). Due to the axial symmetry, the transverse shearing force component ( $Q_\theta$ ), the tangential shearing force components ( $N_{\theta s}$ ,  $N_{s\theta}$ ) and torsional moments ( $M_{s\theta}$ ,  $M_{\theta s}$ ) will vanish.



a) Internal forces on a wall element



b) Internal forces on a circular flat shell element

Figure 1.9 Tank simulation using thin shell element

## 1.5 Analysis of water tanks under static loading

### 1.5.1 Introduction

According to the three standard soil models available in *ELPLA* (simple assumption model - *Winkler's* model - Continuum model), nine numerical calculation methods are considered to analyze the tank considering soil structure interaction as shown in Table 1.2.

Table 1.2 Numerical calculation methods

Method No.	Method
1	Linear contact pressure (Simple assumption model)
2	Constant modulus of subgrade reaction ( <i>Winkler's</i> model)
3	Variable modulus of subgrade reaction ( <i>Winkler's</i> model)
4	Modification of modulus of subgrade reaction by iteration ( <i>Winkler's</i> model/ Continuum model)
5	Modulus of compressibility method for elastic raft on half-space soil medium (Isotropic elastic half-space soil medium - Continuum model)
6	Modulus of compressibility method for elastic base on layered soil medium (Solving system of linear equations by iteration) (Layered soil medium - Continuum model)
7	Modulus of compressibility method for elastic base on layered soil medium (Solving system of linear equations by elimination) (Layered soil medium - Continuum model)
8	Modulus of compressibility method for rigid base on layered soil medium (Layered soil medium - Continuum model)
9	Modulus of compressibility method for flexible base on layered soil medium (Layered soil medium - Continuum model)

The Finite elements-method is used to analyze the tank wall and base for all numerical calculation methods except Continuum model for rigid and flexible bases, which did not obey the elasticity rules. In the Finite elements-analysis, the tank base is represented by annular shell elements according to the dimensional nature of the base.

To formulate the equations of the numerical calculation methods, both the base and the contact area of the supporting medium are divided into annular elements as shown in Figure 1.10. Compatibility between the base and the soil medium in vertical direction is considered for all methods except Simple assumption model.

The fundamental formulation of equilibrium equation for the tank can be described in general form through the following equation:

$$[k_p]\{\delta\} = \{F\} \quad (1.66)$$

where  $\{F\}$  is the vector of forces acting on the tank,  $[k_p]$  is the stiffness matrix of the tank and  $\{\delta\}$  is the deformation vector.

In principle for all calculation methods, the acting forces are known and equal to the applied forces on the tank wall and base, while the reaction forces (contact forces) are required to be found according to each soil model.

It is assumed that the contact pressure  $q_i$  can be replaced by equivalent force  $Q_i$  at the various nodal rings. The contact pressure around the nodal ring  $i$  is given by  $q_i = Q_i/A_i$  over an annular area  $A_i$  corresponding to the nodal contact  $i$ . According to subsoil models (Simple assumption model - *Winkler's* model - Continuum model), six numerical calculation methods are considered to find the contact pressures  $q_i$ , and hence to analyze the tank. The next pages describe the interaction between the tank base and subsoil medium in these methods.

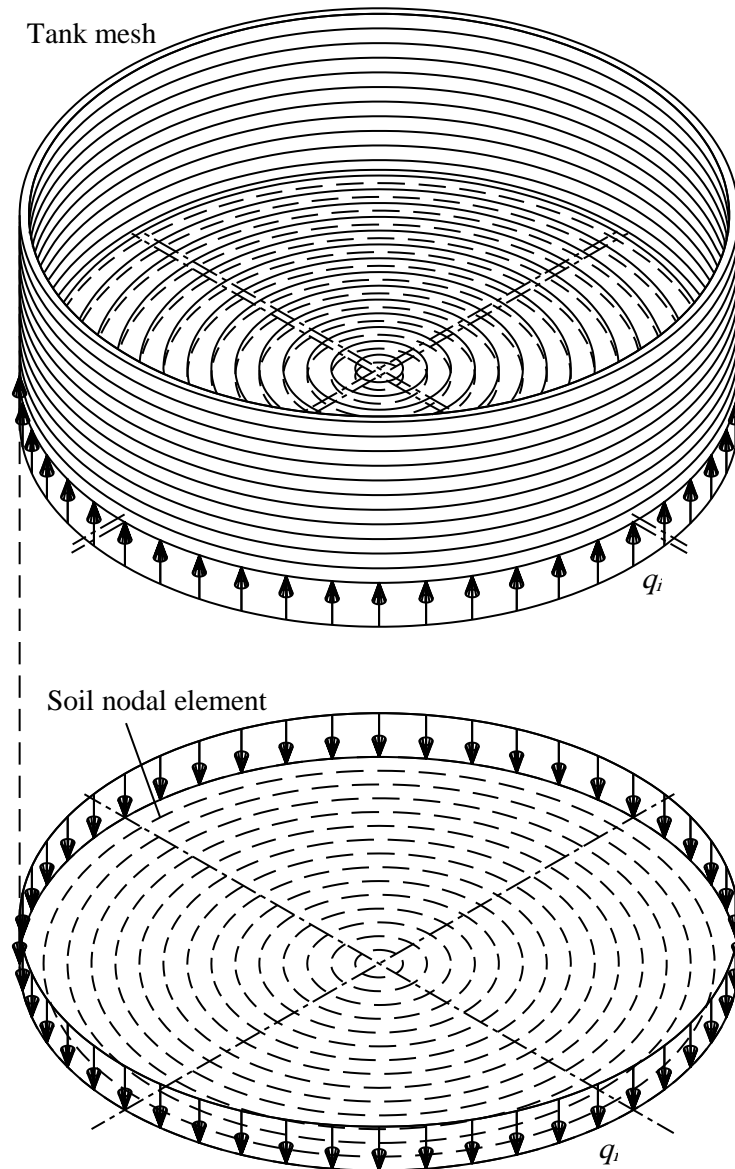


Figure 1.10 Action between tank base and soil

### 1.5.2 Simple assumption model

This method is the simplest one for determination of the contact pressure distribution under the tank base. The assumption of this method is that there is no compatibility between the tank base deflection and the soil settlement. In the method, it is assumed that the contact pressures are distributed uniformly on the bottom of the base (statically determined) as shown in Figure 1.11, in which the resultant of soil reactions coincides with the resultant of applied loads.

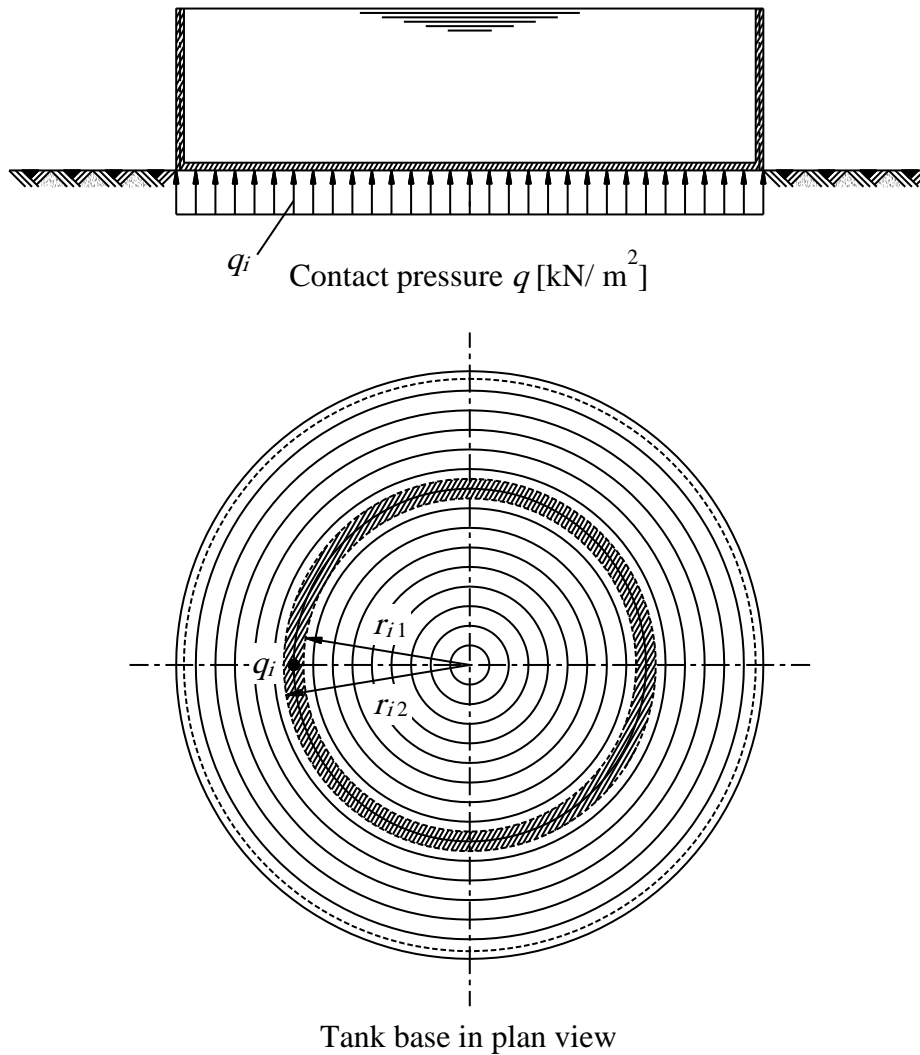


Figure 1.11 Contact pressure distribution for Simple assumption model

For a base without eccentricity the contact pressure  $q_i$  will be uniform under the base and is given by:

$$q_i = \frac{N}{A_b} \quad (1.67)$$

where  $N$  is the resultant force on the tank and  $A_b$  is the area of the tank base.

#### 1.5.2.1 System of equations of Simple assumption model

The tank can be analyzed by calculating the soil reactions at the different nodal rings of the Finite elements-mesh. This is done by obtaining the contact pressure  $q_i$  from equation (1.67). Then, the contact force  $Q_i$  at ring  $i$  is given by:

$$Q_i = q_i (\pi r_{i2}^2 - \pi r_{i1}^2) \quad (1.68)$$

where  $r_{i1}$  and  $r_{i2}$  are the outer and inner radii of the annular element  $i$ , [m].

Considering the entire base, the base will deflect under the action of the total external forces  $\{F\}$  due to known applied loads  $\{P\}$  and the known soil reactions  $\{Q\}$ , where:

$$\{F\} = \{P\} - \{Q\} \quad (1.69)$$

The equilibrium of the system is expressed by the following matrix equation:

$$[k_p]\{\delta\} = \{P\} - \{Q\} \quad (1.70)$$

### 1.5.2.2 Equation solver of linear contact pressure method

As the stiffness matrix  $[k_p]$  in equation (1.66) is a diagonal matrix, the system of linear equations in equation (1.70) is solved by Banded coefficients-technique. The unknown variables are the nodal displacements  $w_i$  and the nodal rotations  $\chi_i$ .

### 1.5.3 Winkler's model

The oldest method for the analysis of foundation on elastic medium is the modulus of subgrade reaction, which was proposed by *Winkler* (1867). The assumption of this method is that the soil model is represented by elastic springs as shown in Figure 1.12. The settlement  $s_i$  of the soil medium at any point  $i$  on the surface is directly proportional to the contact pressure  $q_i$  at that point and is mathematically expressed as:

$$q_i = k_{si} s_i \quad (1.71)$$

The ratio between the contact pressure  $q_i$  [kN/ m<sup>2</sup>] and the corresponding settlement  $s_i$  [m] is termed the modulus of subgrade reaction  $k_{si}$  [kN/ m<sup>3</sup>].

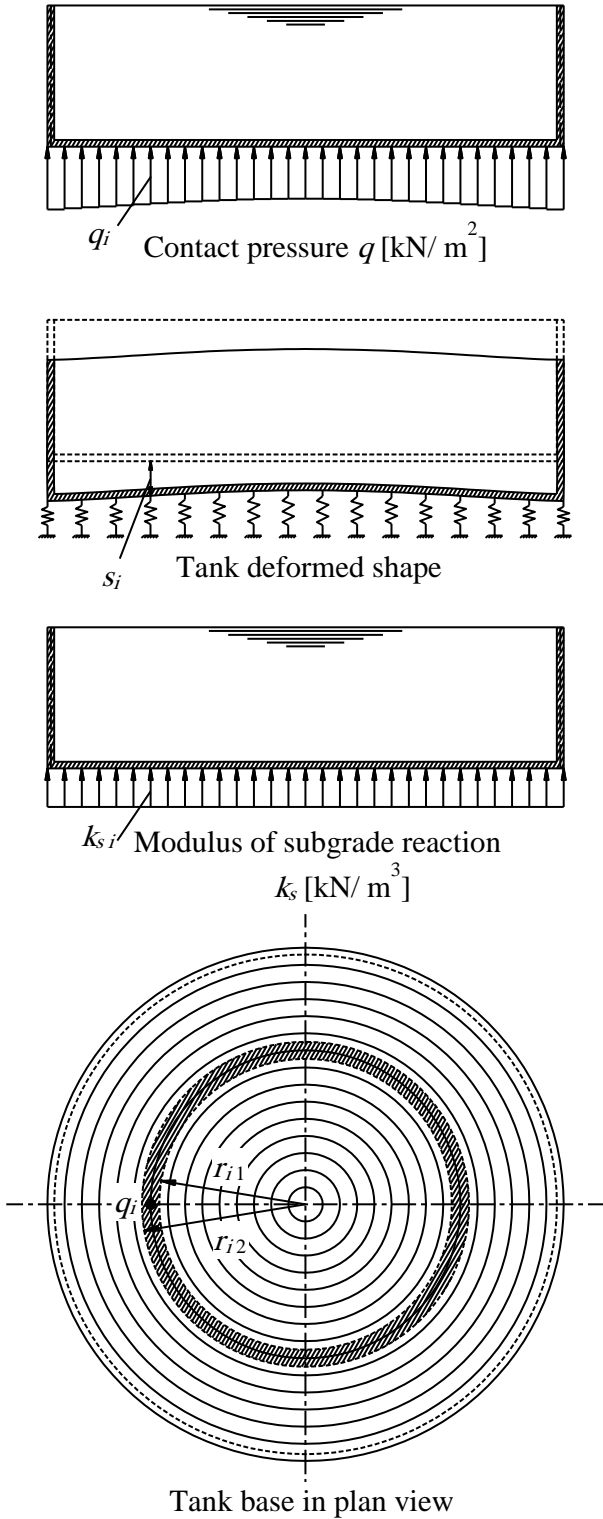


Figure 1.12 Winkler's model

### 1.5.3.1 System of equations of Winkler's model

For a nodal ring  $i$  on the Finite elements-mesh, the contact force  $Q_i$  is given by:

$$Q_i = (\pi r_{i2}^2 - \pi r_{i1}^2) k_{si} s_i \quad (1.72)$$

It should be noticed that  $k_{si}$  is the modulus of subgrade reaction at nodal ring  $i$ . It may be constant for the entire base (Constant modulus of subgrade reaction) or variable from a nodal ring to another (Variable modulus of subgrade reaction).

Considering the entire base, equation (1.72) can be rewritten in matrix form as:

$$\{Q\} = [k_s]\{s\} \quad (1.73)$$

### 1.5.3.2 Complete stiffness formulation of Winkler's model

The base will deflect under the action of the total external forces  $\{F\}$  due to known applied loads  $\{P\}$  and the unknown soil reactions  $\{Q\}$ , where:

$$\{F\} = \{P\} - \{Q\} \quad (1.74)$$

The equilibrium of the tank-soil system is expressed by the following matrix equation:

$$[k_p]\{\delta\} = \{P\} - \{Q\} \quad (1.75)$$

Considering the compatibility of deformation between the base and the soil medium, where the soil settlement  $s_i$  equal to the base deflection  $w_i$ , equation (1.73) for *Winkler's* model can be substituted into equation (1.75) as:

$$[[k_p]+[k_s]]\{\delta\} = \{P\} \quad (1.76)$$

Equation (1.76) shows that the stiffness matrix of the whole tank-base-soil system is the sum of the tank and the soil stiffness matrices,  $[k_p]+[k_s]$ .

### 1.5.3.3 Equation solver of Winkler's model

It should be noticed that the soil stiffness matrix  $[k_s]$  is a purely diagonal matrix for *Winkler's* model. Therefore, the total stiffness matrix for the tank and the soil is a banded matrix. Then, the system of linear equation (1.76) is solved by Banded coefficients-technique. Since the total stiffness matrix is a banded matrix, the Equation solver equation (1.75) takes short computation time by applying this method.

The unknown variables in equation (1.76) are the nodal displacements  $w_i$  ( $w_i = s_i$ ) and the nodal rotations  $\chi_i$ . After solving the system of linear equations (Eq. 4.76), substituting the obtained settlements  $s_i$  in equation (1.73), gives the unknown contact forces  $Q_i$ .

### 1.5.4 *Winkler's/ Continuum model*

This method was proposed by *Ahrens/ Winselmann* (1984), which based on the soil, is represented by variable moduli of subgrade reactions similar to the Continuum model. In the method the base and soil medium are treated separately, the results of one analysis forming the boundary conditions for the subsequent analysis as part of an iterative process. By modifying the variable moduli through the iterative process, the compatibility between the soil and base interface is reached. The obtained results here are similar to those by Continuum model. The method is not only used for analysis of the foundations by Continuum model but also by modulus of subgrade reaction with variable moduli. The first iterative cycle gives an analysis for modulus of subgrade reaction with variable moduli. The results at any intermediate iteration cycle may be considered as acceptable results, which in fact lie between *Winkler's* model with variable moduli and Continuum model. See Figure 1.13.

The iteration process of this method can be described as follows:

i) First, uniform distribution of contact pressure  $q_o$  on the bottom of the foundation is assumed as:

$$q_o = \frac{N}{A_b} \quad (1.77)$$

ii) For a set of nodal rings of Finite elements-mesh, the soil settlement  $s_i$  at nodal ring  $i$  due to contact forces in manner described later for Continuum model is obtained from:

$$s_i^{(j)} = \sum_{k=1}^n c_{i,k} Q_k \quad (1.78)$$

iii) The spring stiffness  $k_i$  from the soil settlement  $s_i$  and contact force  $Q_i$  is computed from:

$$k_i^{(j)} = \frac{Q_i^{(j)}}{s_i^{(j)}} \quad (1.79)$$

iv) The foundation is analyzed as plate on springs, the spring coefficients are used to generate the soil stiffness matrix  $[k_s]$ . This matrix will be a diagonal matrix. Therefore, adding the soil stiffness matrix  $[k_s]$  to the base stiffness matrix  $[k_p]$  is easy. Then, the overall matrix for wall-base-soil system becomes a banded matrix. The entire system equation is expressed as:

$$[[k_p]+[k_s]]\{\delta\} = \{P\} \quad (1.80)$$

v) A set of nodal displacements  $\{\delta\}$  is obtained by solving the system equation (1.80) using the Banded coefficients-technique.

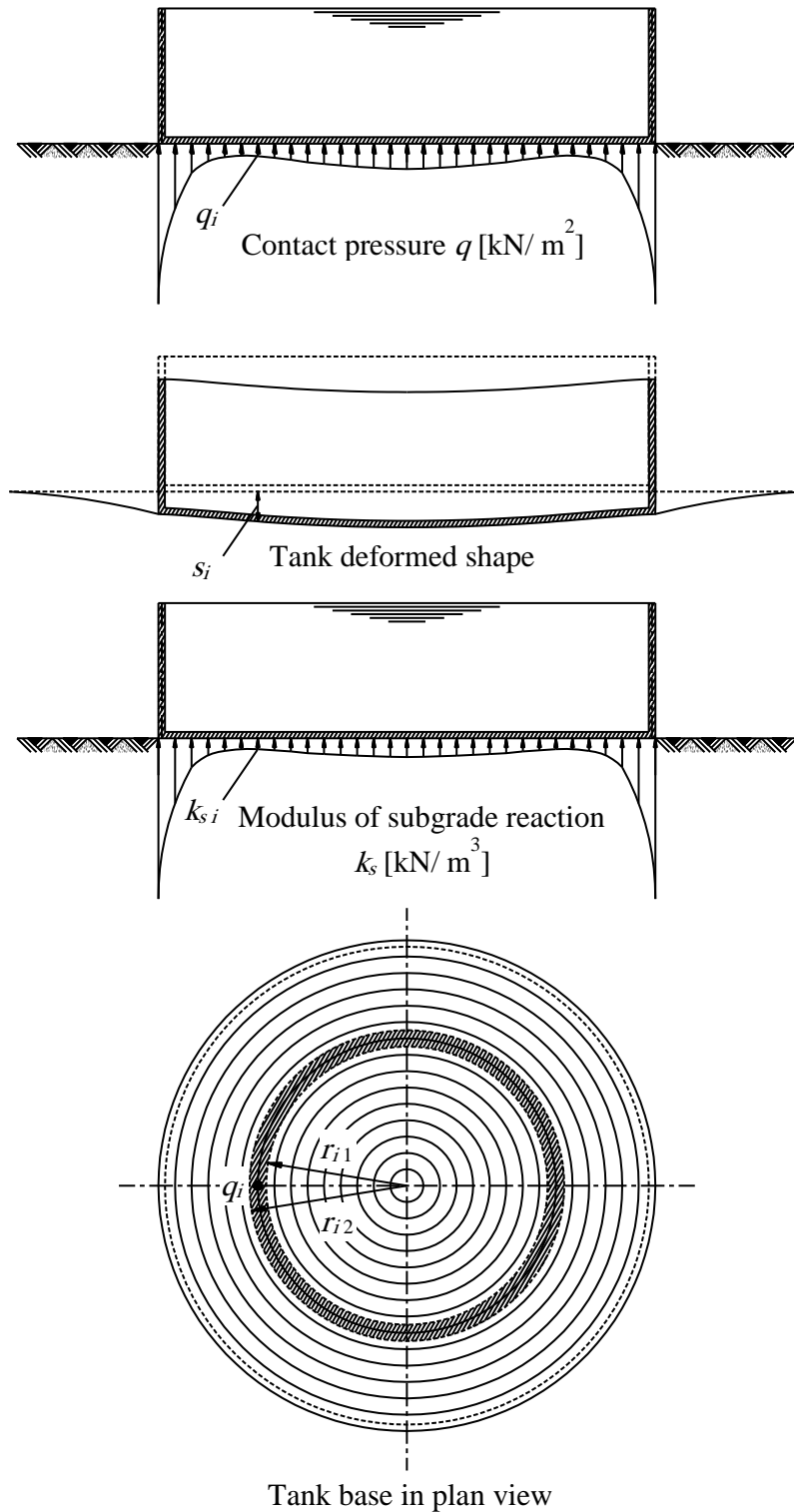


Figure 1.13 Winkler/ Continuum model

## Mathematical model

---

*vi*) The soil settlements  $s_i$  are compared with the corresponding base deflections  $w_i$ , which were computed from the system equation (1.80):

$$\eta = \| s_i - w_i \| \quad (1.81)$$

*vii*) If the accuracy does not reach to a specified tolerance  $\eta$  a new set of contact forces are obtained using:

$$Q_i^{(j+1)} = k_i^{(j)} w_i^{(j)} \quad (1.82)$$

The steps *ii* to *vii* are repeated until the accuracy reaches to a specified tolerance  $\eta$ , which means that sufficient compatibility between the base deflections  $w_i$  and the soil settlements  $s_i$  is reached in the base-soil interface. Figure 1.14 shows the iteration cycle of the iteration process.

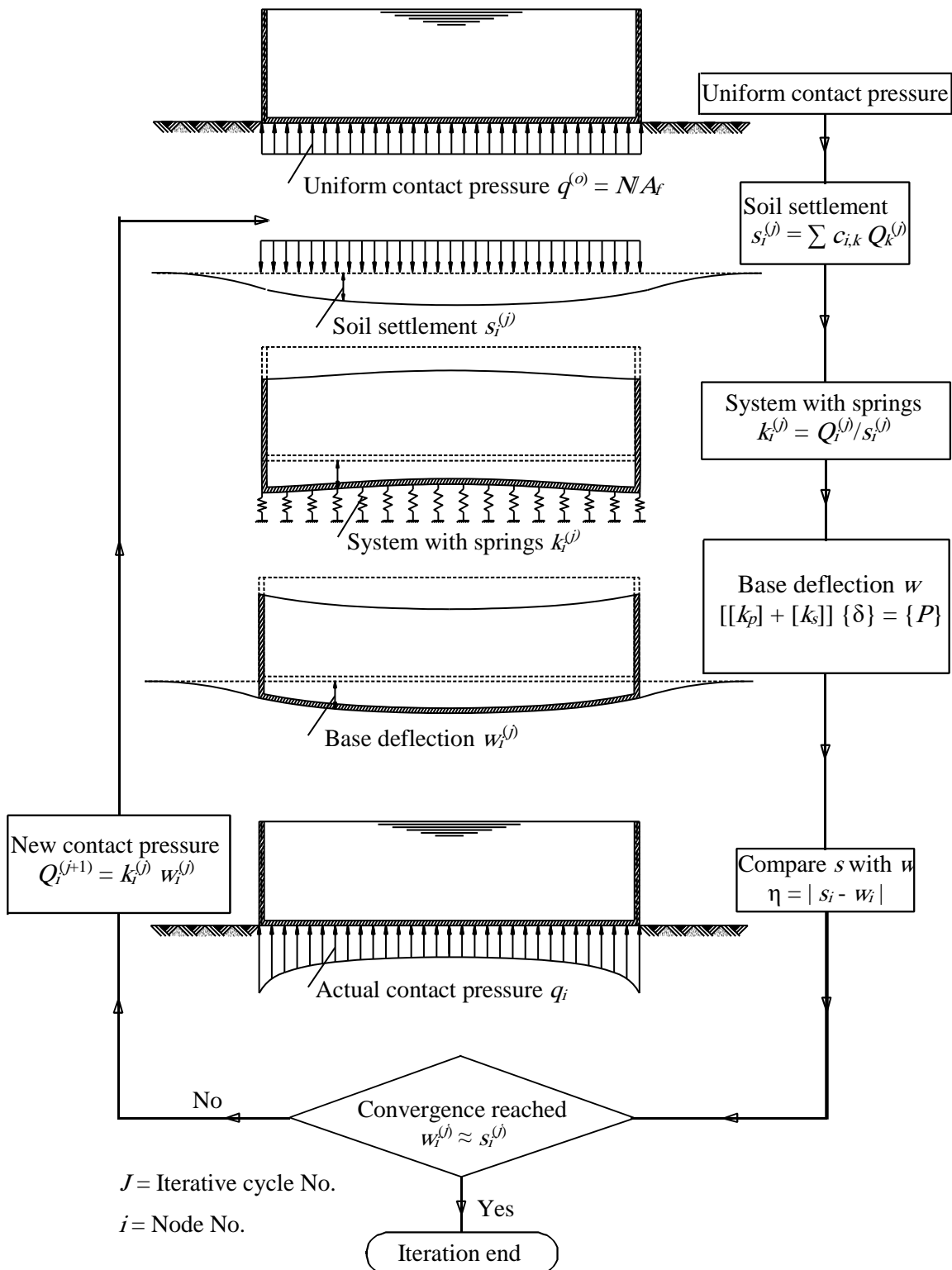


Figure 1.14 Iteration cycle of the iteration process

### 1.5.5 Continuum model for elastic base

Continuum model was first proposed by *Ohde* (1942), which based on the settlement will occur not only under the loaded area but also outside (Figure 1.15). Otherwise, the settlement at any nodal point is affected by the forces at all the other nodal points.

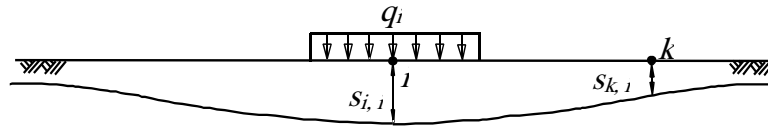


Figure 1.15 Influence line of elastic displacement in Continuum model

Continuum model assumes continuum behavior of the soil, where the soil is represented as isotropic elastic half-space medium or layered medium. Consequently, this model overcomes the assumption of *Winkler's* model, which does not take into account the interaction between the different points of the soil medium. Representation of soil as a continuum medium is more accurate as it realizes the interaction among the different points of the continuum medium. However, it needs mathematical analysis that is more complex. The earliest application for rafts on continuum medium using Finite elements-method related to *Cheung/ Zienkiewicz* (1965). These authors considered the soil as isotropic elastic half-space medium.

The isotropic elastic half-space soil medium bases on *Boussinesq's* solution (1885). The medium in this solution is semi-infinite homogeneous isotropic linear elastic solid subjected to a concentrated force. The force acts normal to the plane boundary at the surface. This basic solution can be used to obtain the surface settlement of isotropic elastic half-space soil medium subjected to a concentrated load acting on the ground surface.

Continuum model for elastic base, which is described here, considers the interaction between the base and soil. It represents the soil as layered soil medium (Figure 1.16).

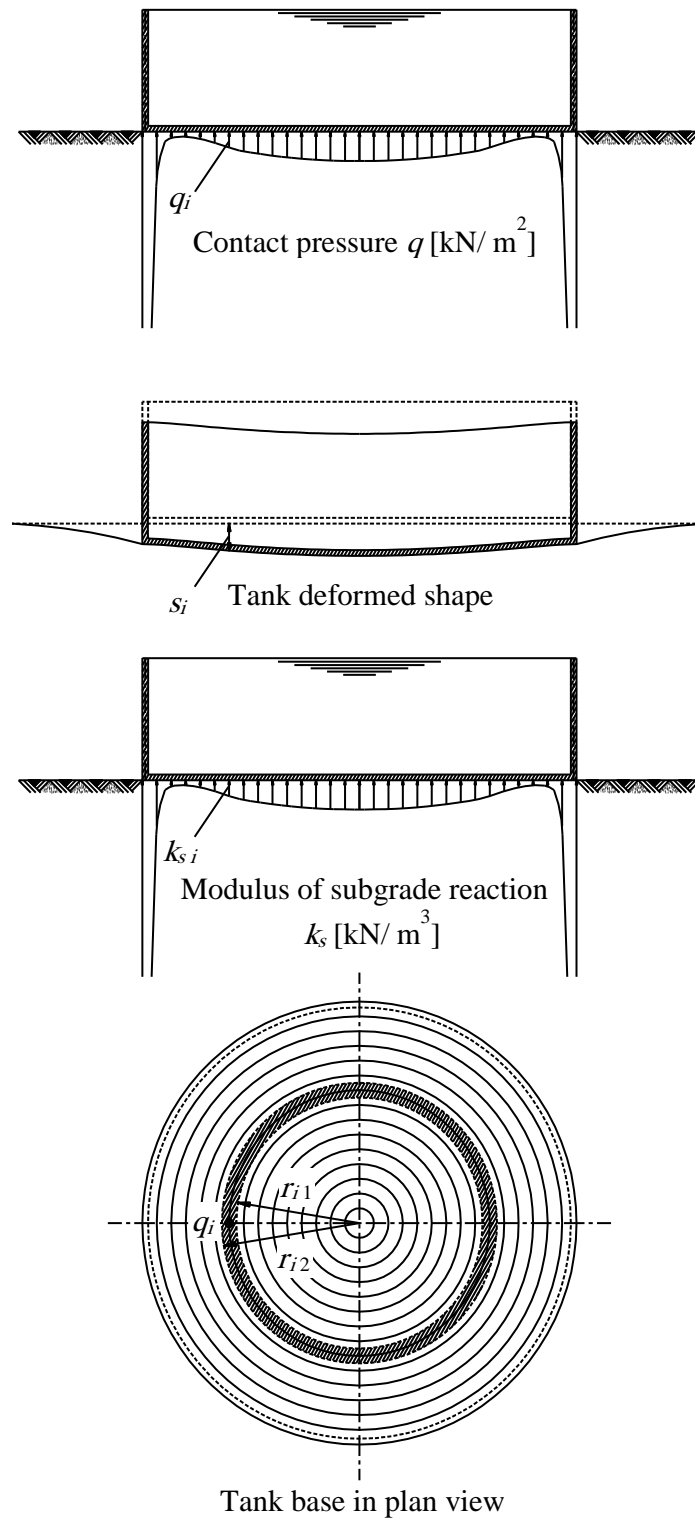


Figure 1.16 Continuum (elastic base) model

**1.5.5.1 Formulation of flexibility matrix of soil**

The settlement  $s_{i, k}$  of the nodal ring  $i$ , due to contact force  $Q_k$  on nodal ring  $k$ , Figure 1.17, can be expressed by:

$$s_{i, k} = c_{i, k} Q_k \tag{1.83}$$

The ratio between the settlement  $s_{i, k}$  of nodal ring  $i$  and the contact force  $Q_k$  at a nodal ring  $k$  is termed the flexibility coefficient  $c_{i, k}$  [m/ kN]. It can be recognized as the settlement of a nodal ring  $i$  due to a unit load at a nodal ring  $k$ .

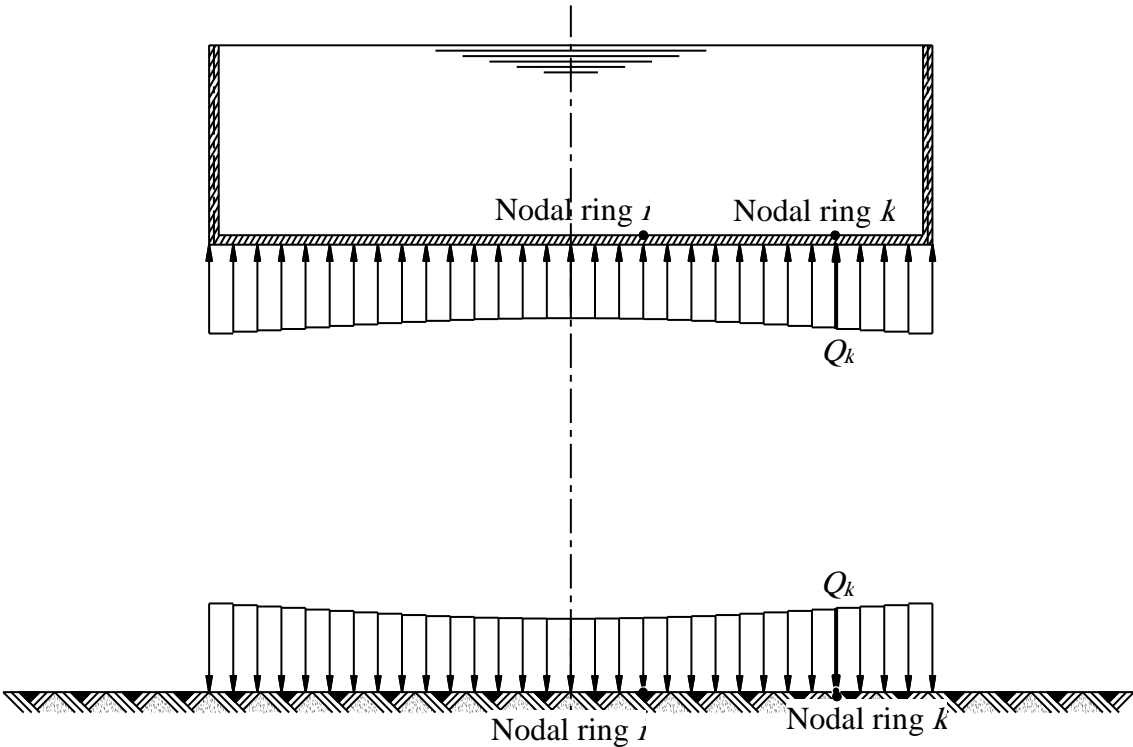


Figure 1.17 Settlement  $s_{i, k}$  of nodal ring  $i$  due to contact force  $Q_k$  at nodal ring  $k$

**1.5.5.2 Assembling of the flexibility matrix**

To find the settlement  $s_i$  at nodal ring  $i$ , equation (1.83) is applied for that nodal ring  $i$ , while equation (1.84) is applied for the other remaining nodal rings considering contact forces over nodal rings. For a set of nodal rings of Finite elements-mesh, the settlement at nodal ring  $i$  is obtained from:

$$s_i = s_{i, 1} + s_{i, 2} + s_{i, 3} + \dots + s_{i, n} = c_{i, 1} Q_1 + c_{i, 2} Q_2 + c_{i, 3} Q_3 + \dots + c_{i, n} Q_n \tag{1.84}$$

Equation (1.85) in series form is:

$$s_i = \sum_{k=1}^n c_{i,k} Q_k \quad (1.85)$$

Equation (1.85) for the entire foundation in matrix form is:

$$\begin{Bmatrix} s_1 \\ s_2 \\ s_3 \\ \vdots \\ s_n \end{Bmatrix} = \begin{bmatrix} c_{1,1} & c_{1,2} & c_{1,3} & \cdots & c_{1,n} \\ c_{2,1} & c_{2,2} & c_{2,3} & \cdots & c_{2,n} \\ c_{3,1} & c_{3,2} & c_{3,3} & \cdots & c_{3,n} \\ \vdots & \vdots & \vdots & \ddots & \vdots \\ c_{n,1} & c_{n,2} & c_{n,3} & \cdots & c_{n,n} \end{bmatrix} \begin{Bmatrix} Q_1 \\ Q_2 \\ Q_3 \\ \vdots \\ Q_n \end{Bmatrix} \quad (1.86)$$

Equation (1.86) is simplified to:

$$\{s\} = [c]\{Q\} \quad (1.87)$$

To assemble the flexibility matrix of the soil  $[c]$ , each node is loaded by a unit contact force and the resulting settlements in all remaining nodal rings and in the loaded rings are calculated. Inverting the flexibility matrix  $[c]$ , gives the  $[n \times n]$  stiffness matrix of the soil  $[k_s]$  corresponding to the contact forces at the  $n$  nodal rings such that:

$$\{Q\} = [k_s]\{s\} \quad (1.88)$$

### 1.5.5.3 Complete stiffness formulation for isotropic elastic half-space soil medium

The base will deflect under the action of the total external forces  $\{F\}$  due to known applied loads  $\{P\}$  and the unknown soil reactions  $\{Q\}$ , where:

$$\{F\} = \{P\} - \{Q\} \quad (1.89)$$

The equilibrium of the wall-base-soil system is expressed by the following matrix equation:

$$[k_p]\{\delta\} = \{P\} - \{Q\} \quad (1.90)$$

Considering the compatibility of deformation between the base and the soil medium, where the soil settlement  $s_i$  is equal to the base deflection  $w_i$ , equation (1.88) for Continuum model can be substituted into equation (1.90) as:

$$[[k_p]+[k_s]]\{\delta\} = \{P\} \quad (1.91)$$

Equation (1.91) shows that the stiffness matrix of the whole wall-base-soil system is the sum of the wall-base and the soil stiffness matrices,  $[k_p] + [k_s]$ .

It should be noticed that the matrix  $[k_s]$  is not compatible with the matrix  $[k_p]$ , because the degrees of freedom in equation (1.88) differ from that in equation (1.90). To overcome this problem, equation (1.88) can be treated by extending the row and column of matrix  $[k_s]$  in the same manner as the matrix  $[k_p]$ . Consequently, the operation of matrix equations can then be accepted.

#### 1.5.5.4 Equation solver for isotropic elastic half-space soil medium

It should be noticed that the matrix  $[k_s]$  is full matrix. Therefore, the total stiffness matrix for the raft and the soil is also full matrix.

The system of linear equations is solved by *Gauss* elimination-technique. Since the total stiffness matrix is a full matrix, the equation solver equation (1.91) takes long computation time by applying this method. The unknown variables in equation (1.91) are the nodal displacements  $w_i$  ( $w_i = s_i$ ) and the nodal rotations  $\chi_i$ . After solving the system of linear equation (1.91), substituting the obtained settlements  $s_i$  in equation (1.88), gives the unknown contact forces  $Q_i$ .

### 1.5.6 Continuum model for rigid base

In many practice cases, treating the tank as completely rigid is convenient. In this case, for a tank with symmetrical shape and loading, the unknowns of the interaction problem, Figure 1.18, are:

- $n$  contact pressures  $q_i$ .
- Rigid body translation of the raft  $w_o$  at the centroid.

#### 1.5.6.1 Formulation of the rigid raft

To describe the method, consider the base shown Figure 1.18. The contact pressure  $q_i$  at a nodal ring  $i$  under the base is replaced by equivalent contact force  $Q_i$ . For a set of nodal rings of elements-mesh, the settlement at a nodal ring  $i$  is obtained from:

$$s_i = \sum_{k=1}^n c_{i,k} Q_k \quad (1.92)$$

Considering the entire base, equation (1.92) can be rewritten in matrix form as:

$$\{s\} = [c]\{Q\} \quad (1.93)$$

Inverting the flexibility matrix  $[c]$ , gives the stiffness matrix of the soil  $[k_s]$  corresponding to the contact forces at the  $n$  nodal rings such that:

$$\{Q\} = [k_s]\{s\} \quad (1.94)$$

For a tank with symmetrical load and shape, the settlement will be uniform ( $s_i = w_o$ ) and the tank will not rotate ( $\chi_o = 0$ ). Therefore, the unknowns of the problem reduce to  $n$  contact pressures  $q_i$  and rigid body translation  $w_o$ .

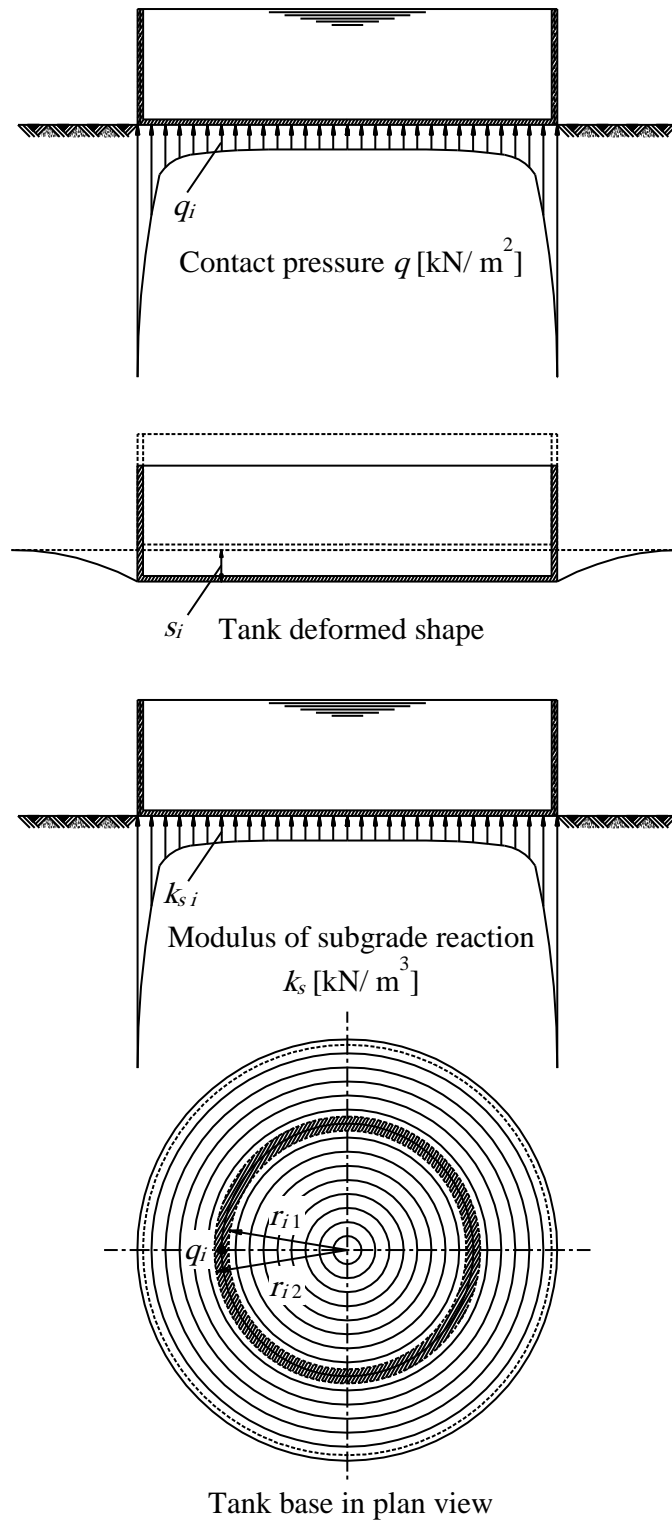


Figure 1.18 Continuum (rigid base) model

### 1.5.6.2 Derivation of uniform settlement $w_o$

The derivation of the uniform settlement for the rigid base can be carried out by equating the settlement  $s_i$  by uniform settlement  $w_o$  for all nodal rings in equation (1.94) In this case, the contact forces can be rewritten as a function in the terms  $k_{i,j}$  of the soil stiffness matrix as follows:

$$\left. \begin{aligned} Q_1 &= k_{1,1} w_o + k_{1,2} w_o + k_{1,3} w_o + \dots + k_{1,n} w_o \\ Q_2 &= k_{2,1} w_o + k_{2,2} w_o + k_{2,3} w_o + \dots + k_{2,n} w_o \\ Q_3 &= k_{3,1} w_o + k_{3,2} w_o + k_{3,3} w_o + \dots + k_{3,n} w_o \\ &\vdots \\ Q_n &= k_{n,1} w_o + k_{n,2} w_o + k_{n,3} w_o + \dots + k_{n,n} w_o \end{aligned} \right\} \quad (1.95)$$

Carrying out the summation of the all contact forces:

$$\sum_{i=1}^n Q_i = w_o \sum_{i=1}^n \sum_{j=1}^n k_{i,j} \quad (1.96)$$

The rigid body translation  $w_o$ , which equals to the settlement  $s_i$  at all nodal rings, is obtained from:

$$w_o = \frac{\sum_{i=1}^n Q_i}{\sum_{i=1}^n \sum_{j=1}^n k_{i,j}} = \frac{N}{\sum_{i=1}^n \sum_{j=1}^n k_{i,j}} \quad (1.97)$$

Substituting this value of  $w_o$  in equation (1.94) gives the  $n$  unknown contact forces  $Q_i$ .

The summation of terms  $k_{i,j}$  ( $= N/ w_o$ ) may be used to determine the modulus of subgrade reaction  $k_s$ .

### 1.5.7 Continuum model for flexible base

If the tank base is perfectly flexible, then the contact stress will be equal to the gravity stress exerted by the base on the underlying soil. See Figure 1.19.

For the set of nodal rings of the base, the soil settlements are:

$$\{s\} = [c]\{Q\} \quad (1.98)$$

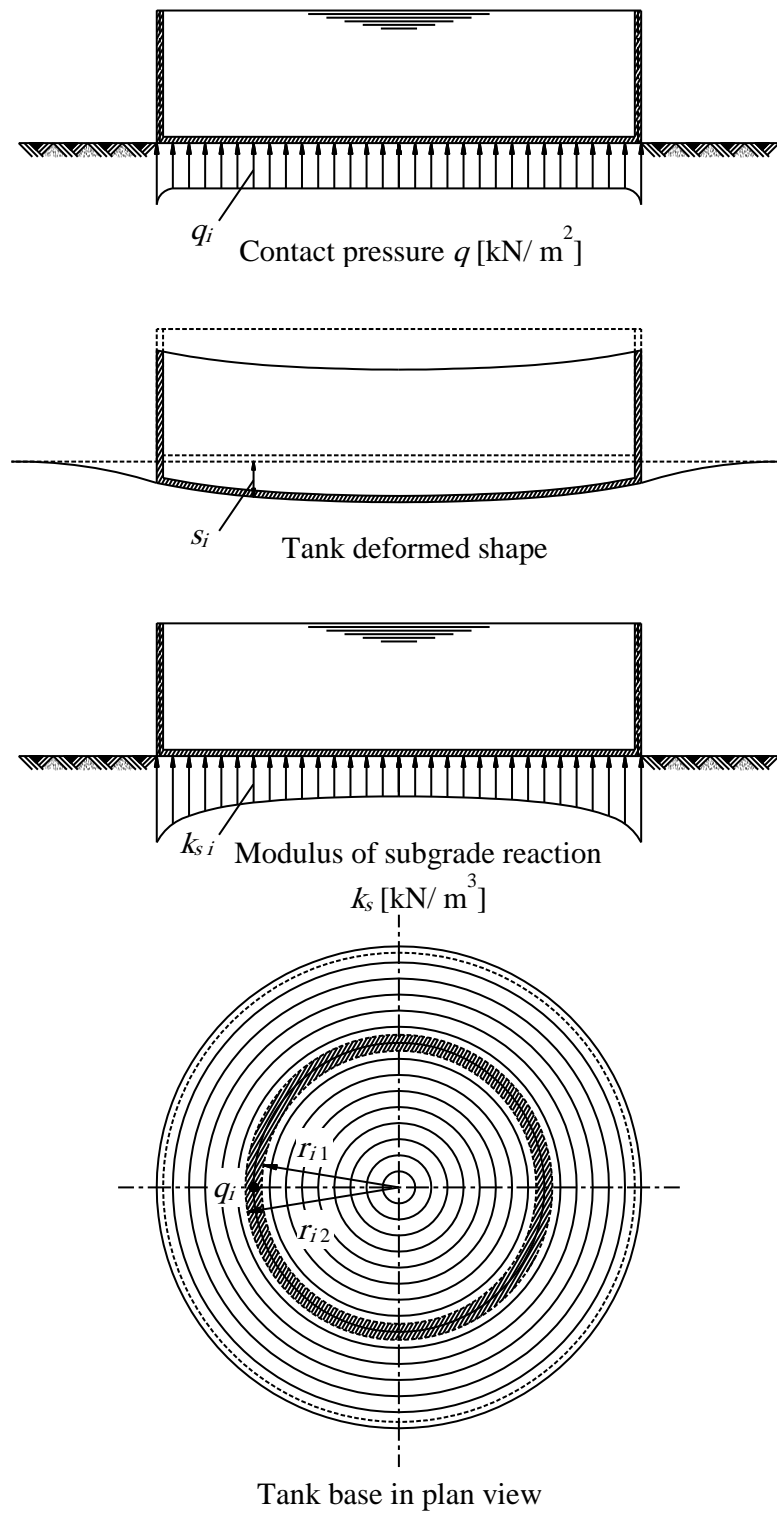


Figure 1.19 Continuum (flexible base) model

## 1.6 Reference

- [1] *Ahrens, H. and Winselmann, D.* (1984): "Eine iterative Berechnung von Flächengründungen nach dem Steifemodulverfahren". Finite Elemente Anwendungen in der Baupraxis Verlag W. Ernst & Sohn, München.
- [2] *Bakhoun, M.* (1992): "Structural Mechanics". Cairo, Egypt.
- [3] *Booker, J. R. and Small, J. C.* (1983): "The analysis of liquid storage tanks on deep elastic foundation". Int. J. Numer. Anal. Methods Geomech. 7, 187-207.
- [4] *Borowicka, H.* (1939): Druckverteilung unter elastischen Platten, Ingenieur-Archiv, Band 10, S. 113-125.
- [5] *Das, B. M.* (1997): "Advanced soil mechanics", 2nd ed., USA, Tailor & Francis.
- [6] *El Gendy M. and El Gendy A.* (2015): "Analysis and Design of Slab Foundations by FE-Method- Program *ELPLA 10*". GEOTEC Software Inc., Canada.
- [7] *El Gendy, M.* (2003): "Numerical Modeling of Rigid Circular Rafts on Consolidated Clay Deposits". Int. Workshop on Geotechnics of Soft Soils-Theory and Practice. Vermeer, Schweiger, Karstunen & Cudny (eds.).
- [8] *El Gendy, M.* (2006): "Developing stress coefficients for raft-deformation on a thick clay layer". Vol. 41, No. 3, September 2006, pp. 73-108. Scientific Bulletin, Faculty of Engineering, Ain Shams University, Cairo, Egypt.
- [9] *El Gendy, O.* (2016): "Behavior of Tanks under Static and Cyclic Loading". MSc Thesis, Port Said University.
- [10] *EL Mezaini, N.* (2006): "Effects of soil-structure interaction on the analysis of cylindrical tanks". Practice periodical on structural design and construction, Vol. 11, No. 01, Pages 50 -57.
- [11] *Ghali, A.* (2000): "Circular storage tanks and silos – 2<sup>nd</sup> edition", by E & FN spon – 11 New Fetter Lane, London EC4P 4EE.
- [12] *Godbout, S./ Marquis, A./ Fafard, M./ Picard, A.* (2003): Analytical determination of internal forces in a cylindrical tank wall from soil, liquid, and vehicle loads, Canadian Biosystems Engineering/Le génies des biosystèmes au Canada 45: 5.7-5.14.
- [13] *Grafton, P. E. and Strome, D. R.* (1963): "Analysis of Axis-Symmetric Shells by the Direct Stiffness Method," AIAA Journal, Vol. 1, No. 10, pp. 2342-2347.
- [14] *Graßhoff, H.* (1955): "Setzungsberechnungen starrer Fundamente mit Hilfe des kennzeichnenden Punktes". Der Bauingenieur, S. 53-54.

- 
- [15] *Hauso, A.* (2014): "Analysis methods for thin concrete shells of revolution", M.Sc. Thesis, Faculty of Engineering, Norwegian University of Science and Technology.
- [16] *Hemsley, J. A.* (1998): "Elastic analysis of raft foundations", Thomas Telford Ltd, 1 Heron Quay, London.
- [17] *Hibbitt, Karlsson and Sorenson* (2008): "ABAQUS 6.8: A computer software for finite element analysis", *Hibbitt, Karlsson and Sorenson Inc.*, Rhode Island, USA.
- [18] *Houchmand Naïmi* (1957): Beiträge zur Anwendung der Schalentheorie bei Bogenstaumauern, Promotionsarbeit, Eidgenössischen Technischen, Hochschule in Zürich.
- [19] *Kany, M.* (1974): "Berechnung von Flächengründungen", 2. Auflage Verlag Ernst & Sohn, Berlin.
- [20] *Kany, M., El Gendy M. and El Gendy A.* (2008): "Analysis and Design of Slab Foundations by FE-Method- Program *ELPLA 9.2*". GEOTEC Software, Zirndorf, Germany.
- [21] *Karaşin, H./ Gülkan, P./ Aktas, G.* (2014): A Finite Grid Solution for Circular Plates on Elastic Foundations, *KSCCE Journal of Civil Engineering* (2015) 19(4):1157-1163.
- [22] *Kukreti, A. & Siddiqi, Z.* (1997): "Analysis of fluid storage tanks including foundation-superstructure interaction using differential quadrature method". *Appl. Math. Modeling* 1997, 21:193-205, April.
- [23] *Kukreti, A., Zaman, M. and Issa, A.* (1993): "Analysis of fluid storage tanks including foundation-superstructure interaction". *Appl. Math. Modelling* 1993, Vol. 17, December.
- [24] [Mathworld.wolfram.com](http://Mathworld.wolfram.com)
- [25] *Melerski, E. S.* (1991), "Simple elastic analysis of axisymmetric cylindrical storage tanks", *Journal of Structural Engineering*, Vol. 117, No. 11, Pages 3239-3260.
- [26] *Melersky, E.* (2006): "Design analysis of beams, circular plates and cylindrical tanks on elastic foundations – 2<sup>nd</sup> edition". Taylor & Francis group, London, UK.
- [27] *Mistríková, Z & Jendželovský, N* (2012): "Static analysis of the cylindrical tank resting on various types of subsoil", *Journal of civil engineering and management*, Vol. 18(5): 744-751.
- [28] *Mobarak, W.* (2010): "Effect of Tie Girders on Piled Footing in Port Said", M.Sc. Thesis, Faculty of Engineering, Suez Canal University.
- [29] *Nishida, Y.* (1956): "A brief note on compression index of soils". *Journal of SMFE Div., ASCE*, July, p 1027 (1-14).

- [30] *Ohde, J.* (1942): "Die Berechnung der Sohldruckverteilung unter Gründungskörpern Der Bauingenieur". Heft 14/16, S. 99-107 - Heft 17/18 S. 122-127.
- [31] *Percy, J. H., Pian, T. H. H., Klein, S., and Navaratna, D. R.* (1965): "Application of matrix displacement method to linear elastic analysis of shells of revolution." *AIAA Journal*, Vol. 3, No. 11, pp. 2138-2145.
- [32] *Reda, A.*(2009): "Optimization of Reinforced Concrete Piled Raft", M.Sc. Thesis, Faculty of Engineering, Suez Canal University.
- [33] *Rockey, K. C., Evans, H. R., Griffiths, D. W. and Nethercot, D. A.* (1975): "The Finite Element Method- A Basic Introduction For Engineers", by Crosby Lockwood Staples, London.
- [34] *Samangany, A.Y., Naderi R., Talebpur M. H. and Shahabi H.* (2013): "Static and Dynamic Analysis of Storage Tanks Considering Soil-Structure Interaction", *International Research Journal of Applied and Basic Sciences*, Vol. 6(4), 515-532.
- [35] *Szilar, R., Ziesing and Pickhardt* (1986): "Basic- Programme für Baumechanik und Statik". Wilhelm Ernst und Sohn Verlag für Architektur und technische Wissenschaften, Berlin.
- [36] *Terzaghi, K., Peck, R.B. and Mesri, Gh.* (1996), "Soil mechanics in engineering practice", 3rd Ed., John Wiley, New York.
- [37] *Timoshenko, S. & Woinowsky-Krieger S.* (1959): "Theory of plates and shells". McGraw- Hill Book Co. Singapore.
- [38] *Utku, M., and Inceleme, I.* (2000): The Analysis of the Stability of General Slip Surfaces, *Geotechnique*, 15(1): 79-93.
- [39] *Ventsel, E. and Krauthammer, T.* (2001): "Thin Plates and Shells: Theory, Analysis and Applications". Marcel Dekker, INC., New York.
- [40] *Vichare, S. & Inamdar, M.* (2010): "An analytical solution for cylindrical concrete tank on deformable soil", *International journal of advanced structural engineering*, Vol. 2, No. 1, Pages 71-93, Islamic Azad university, south Tehran branch.
- [41] *Winkler, E.* (1867): " Die Lehre von der Elastizität und Festigkeit". Dominicus, Prag.
- [42] [www.wolframalpha.com/entities/plane\\_curves](http://www.wolframalpha.com/entities/plane_curves).
- [43] *Zaman, M. and Koragappa, N.* (1989): "Analysis of tank-foundation-half-space interaction using an energy approach". *Appl. Math. Modelling*, Vol. 13, February.
- [44] *Zienkiewicz, O. C. and Cheung, Y. K.* (1965): "Plates and Tanks on Elastic Foundations - an Application of Finite Element Method". *International Journal of Solids Structures* Vol. 1, pp. 451-461, Pergamon.

- [45] *Zienkiewicz, O. C. and Cheung, Y. K. (1967): "The Finite Element Method in Structural and Continuum Mechanics".* Berkshire, England, by McGraw-Hill Publishing Company Limited.
- [46] *Zienkiewicz, O. C. and Taylor, R. L. (1967): "The Finite Element Method – Vol. 2: Solid Mechanics".* Berkshire, England, by McGraw-Hill Publishing Company Limited.
- [47] *Zingoni, A. (1997): "Shell Structures in Civil and Mechanical Engineering".* Thomas Telford publisher, Thomas Telford services Ltd, 1 Heron Quay, London E14 4JD.